signal for the small fraction of Ad4BP/SF-1 that has entered the nucleolus to get out.

DAX-1 is able to interact directly with Ad4BP/SF-1 (31). The amino-terminal region of DAX-1 contains an interaction domain for Ad4BP/SF-1, and the C terminus of DAX-1 is itself transcriptionally silencing. In addition to the recruitment of corepressors like N-CoR, this silencing C terminus may be the second mechanism by which DAX-1 inhibits Ad4BP/SF-1 transactivation. This silencing carboxyl terminus also correlates with naturally occurring AHC mutations. Coexistence of GFP-DAX-1 and YFP-Ad4BP/SF-1 dramatically changed the fluorescence pattern of both proteins from diffuse distributions to the formation of clear dots, with the two fluorescence signals completely overlapping. The FRAP data in this study revealed that the intranuclear mobility of Ad4BP/SF-1 was also affected upon interaction with DAX-1.

Agonist-bound nuclear receptors form nuclear matrix-bound foci and are believed to be capable of undergoing rapid exchange. As an example, E2 treatment leads ER and the cofactor SRC-1 to strongly interact with the nuclear matrix, after which ER is partially immobilized, possibly representing interaction with more immobilized components of the nuclear structure. Ligand-bound ER and SRC-1 are still capable of rapid recovery within seconds of photobleaching. In the case of an ER antagonist, ER is extremely immobilized with no appreciable photobleaching recovery for several minutes at least, and this immobilization provides a new explanation for the inhibitory effects of the ER antagonist (21). The orphan receptor Ad4BP/SF-1 was also found to be quite mobile within the nucleus, with a mean recovery $t_{1/2}$ of around 0.8 sec after photobleaching. DAX-1 had a very different effect on Ad4BP/SF-1 with respect to the intranuclear mobility. Coexpression of DAX-1 resulted in clearly reduced mobility of Ad4BP/SF-1. These data, together with the result that Ad4BP/SF-1 and DAX-1 undergo the formation of colocalized dots upon interacting with each other, suggest that Ad4BP/SF-1 might be tightly bound to some special structure in the nuclear matrix upon binding with DAX-1. DAX-1 might work as an anchor protein mediating the sharp immobilization of Ad4BP/SF-1 in the nuclear matrix structure. Protein-protein interaction might affect the intracellular mobility of some steroid receptor and thereby contribute to their biological activity.

However, forskolin treatment enabled Ad4BP/SF-1 to recover from the transactivation suppression induced by DAX-1 as evidenced by the luciferase assay and by the fact that the complete overlapping of Ad4BP/SF-1 and DAX-1 signals was partially separated upon PKA activation. This was further supported by the FRAP data showing that the DAX-1-reduced mobility of Ad4BP/SF-1 was rescued by the activation of PKA. These data collectively suggest that activation of PKA may weaken the interaction between DAX-1 and Ad4BP/SF-1 and may disassemble DAX-1 from Ad4BP/SF-1, thus leading to the recovery of Ad4BP/SF-1 transcriptional activity. A previous study also demonstrated that the presence or absence of DAX-1 could not change the SF-1-SF-1-responsive element EMSA result (31). This means that, although DAX-1 can bind directly to SF-1, when SF-1 is activated and binds to the promoters of target genes, it is SF-1 alone, not in combination with DAX-1, that binds to the DNA, *i.e.* DAX-1 must now be stripped from binding with SF-1.

In the Ad4BP/SF-1 amino acid sequence, two regions were determined to be important for the interaction with DAX-1 (11). One is termed the R domain, which is between amino acids 437 and 447, and the other is residue 226 to 230 (ELILQ) of Ad4BP/SF-1. It is intriguing that the interaction between Ad4BP/SF-1 and the coactivator SRC-1 also requires the same residues (ELILQ), leading to the logical deduction that Ad4BP/SF-1-DAX-1 binding and Ad4BP/SF-1-coactivator binding may be mutually competitive, *i.e.* the Ad4BP/SF-1-interacting coactivator-repressor balance may determine the transactivation ability of Ad4BP/SF-1. Based on our present study, activation of the PKA signal pathway leads to the recruitment of the GCN5/TRRAP coactivator complex, and also to the disassembly of the inhibitory DAX-1, both of which may finally direct the coactivator-repressor balance to favoring the activation of Ad4BP/SF-1.

Collectively, activation of PKA can assemble Ad4BP/SF-1 to an active state, as manifested by foci formation, and this process is accompanied by the recruitment of coactivators GCN5/TRRAP, which might represent a newly identified cofactor complex for Ad4BP/SF-1. Direct interaction between Ad4BP/SF-1 and the repressor DAX-1 was visualized as completely overlapping fluorescent dots, and DAX-1 sharply immobilized Ad4BP/SF-1 upon binding. Activation of PKA was able to disrupt or weaken the interaction between DAX-1 and Ad4BP/SF-1 and therefore rescue the Ad4BP/SF-1 transactivation capability. In conclusion, activation of PKA may reintegrate the protein-protein interactions between Ad4BP/SF-1 and its coactivators and repressor, which finally decide the Ad4BP/SF-1 transactivation capability.

MATERIALS AND METHODS

Cell Culture

The human ovarian granulosa-like tumor cell line KGN was originally established by our group and expresses a high level of aromatase activity that is PKA dependent (47); the cells also highly express Ad4BP/SF-1 (48). The cells were maintained in DMEM/Nutrient Mixture F-12, Life Technologies, Inc., Gaithersburg, MD) supplemented with 10% fetal bovine serum, 10 U/liter penicillin, and 10 μg/ml streptomycin in an atmosphere of 5% CO_2 at 37 C. NIH-3T3 and CV1 cells were obtained from American Type Culture Collection (Manassas, VA) and maintained in DMEM supplemented with 10% fetal bovine serum, 10 U/liter penicillin and 10 μg/ml streptomycin in 75-cm^2 flasks at 37 C in 5% CO_2.

Plasmid Constructions

A full-length human Ad4BP/SF-1 cDNA was cloned from a human spleen cDNA library (BD Bioscience CLONTECH, Palo Alto, CA) by PCR using primers based on the human Ad4BP/SF-1 cDNA sequence (GenBank accession no. NM 004959.2). The PCR was performed using an Advantage cDNA PCR kit (BD Bioscience CLONTECH) and an automated thermo-cycler (Whatman Biometra, Gottingen, Germany) with the appropriate program. The PCR product was first subcloned into the pGEM-T-Easy vector (Promega Corp., Madison, WI) and sequenced to validate its structure using an ABI PRIM 377 DNA sequencer (PE Applied Biosystems, Foster City, CA). Finally, Ad4BP/SF-1 cDNA was subcloned into the expression vector pcDNA3.1 (+) (Invitrogen, San Diego, CA) at the *Not*I and *Xba*I restriction sites to produce pcDNA 3.1-Ad4BP/SF-1.

A mutant human Ad4BP/SF-1 cDNA construct containing the G35E mutation found in the patient (8) was made using a QuikChange site-directed mutagenesis kit (Stratagene, La Jolla, CA). Full-length cDNAs of wild-type and mutant Ad4BP/SF-1 were then subcloned into the *Sac*II sites of both pEGFP-C1 and pEYFP-C1 (CLONTECH Laboratories, Inc.), downstream of the humanized GFP or YFP sequence. The boundary regions between GFP (or YFP) and the human Ad4BP/SF-1 cDNAs were sequenced to validate that the Ad4BP/SF-1 cDNAs were placed in the reading frame of GFP or YFP. A human full-length DAX-1 expression vector pRc/RSV-DAX-1 was prepared as previously described (49). The expression plasmids for GFP-DAX-1 chimeras were constructed by inserting the full-length DAX-1 cDNA into the *Hin*dIII and *Xba*I sites of pEGFP-C3 (CLONTECH Laboratories, Inc.). Expression vectors pcDNA3-GCN5 and pcDNA3-TRRAP were constructed previously (30). To make GFP-GCN5, the full-length GCN5 cDNA was inserted into the *Eco*RI-*Xba*I sites of pEGFP-C2, downstream of the fluorescence protein. Chimeras for TRRAP-GFP, TRRAP-YFP, and TRRAP-CFP were prepared by inserting the full-length TRRAP cDNA into the *Eco*RI site of pEGFP-N1, pEYFP-N1, and pECFP-N1, respectively, in which TRRAP was fused to the N terminus of the fluorescent proteins. The firefly luciferase reporter vector pGL3-ArPII construct containing a 1.0-kb human cytochrome P450 CYP19 ArPII was described previously (50).

Relative Luciferase Reporter Assay

On the first day, 1.5×10^5 cells per well in 1 ml growth medium were seeded into 12-well plates. On the second day, 0.8 μg of PGL3-ArPII, 2.0 ng of phRL-CMV, and a total amount of 0.15μg of expression vectors for human Ad4BP/SF-1, chimerical fluorescent protein-Ad4BP/SF-1, or Ad4BP/SF-1 plus other plasmids such as DAX-1, GCN5, TRRAP, or their fluorescent protein chimerical plasmids were transiently cotransfected to each well using the Superfect transfection reagent (QIAGEN, Valencia, CA) following the manufacturer's protocol. For coexpression studies, the total amount of plasmid DNA added to each well was equalized by the addition of empty vector. On the third day, the culture medium was replaced with fresh medium in the presence or absence of 10^{-6} mol/liter forskolin (Sigma-Aldrich Corp., St. Louis, MO). On the fourth day, the cells were lysed in 100 μl/well passive lysis buffer, and the luciferase assay was performed in accordance with the protocol of the Dual-Luciferase Reporter Assay System, using a Lumat LB 9507 luminometer (Berthold Technologies, Bad Wildbad, Germany). The firefly luciferase activity produced by PGL3-ArPII in identically treated triplicate samples was normalized for the renilla luciferase activity produced by phRL-CMV. The data shown are representative of at least three independent experiments.

Living-Cell Laser Confocal Fluorescence Microscopy and FRAP

On the first day, 3×10^5 KGN cells were seeded in 35-mm glass-based dishes (IWAKI, Asahi Techno Glass, Chiba, Japan). On the second day, a total amount of 0.5 μg/dish of various test chimera plasmids was transfected into cells using Superfect. Four hours post transfection, the culture medium was replaced with fresh medium in the presence or absence of 10^{-6} mol/liter forskolin. After overnight incubation (12 h), cells were observed using an LSM 510 META microscope (Carl Zeiss) equipped with a Plan-Apochromat $\times$100 1.4 oil objective.

Transient transfected proteins will potentially cause artifacts from overexpression. Transient transfection also results in a clear cell-to-cell difference of XFP-fusion protein expression level within the same cell population. To roughly overcome these complications, a reference system relating the overexpression level of GFP-X to the endogenous X expression level was established by a quantitative immunofluorescence staining. As a brief example, GFP-DAX-1 is at first transfected to KGN cells, which on the next day was subjected to immunostaining by an anti-DAX-1 antibody and an Alexa Fluor 546-sec antibody. The Alexa Fluor 546 intensity between transfected cells (bearing GFP signal; Alexa Fluor 546 intensity represents both GFP-DAX-1 and endogenous DAX-1), and nontransfected cells (Alexa Fluor 546 intensity represents only endogenous DAX-1) were compared quantitatively and a reference of respective GFP intensity was established. Only cells expressing less than 10-fold [which is usually believed to be near physiological (21)] of endogenous protein level were selected for imaging.

For single fluorescent protein imaging, GFP or YFP fluorescence was excited by the 488-nm or 514-nm laser line, respectively, from an air-cooled fiber-coupled argon laser. For simultaneous imaging of GFP and YFP, a 488-nm laser line was used for excitation, and detection spectrum range was from 491–576 nm. For simultaneous imaging of GFP, YFP, and CFP, a 458-nm laser line was used for excitation, and detection spectrum range was set from 458–587 nm. Raw imagines obtained in a λ-mode were subjected to the META Unmixing procedure to de-mix GFP, YFP, and CFP signals. The reference spectrums for each XFPs were made by imaging cells solely expressing each respective XFP. For GFP, YFP, CFP trilocalization imagining, all three references spectrums were applied for META Unmixing, whereas only GFP and YFP reference spectrums were applied to unmix the GFP and YFP bilocalization images.

Matching the expression levels of proteins being cotransfected is essential to observing a reasonable subcellular interaction. For cotransfection, the amount of each XFP-fusion plasmid was equivalent on a molar basis. During simultaneous multiimaging, cells that express a similar intensity of each fluorescence protein were selected for further study. Parameters such as the laser power, laser line, dichroic beam splitter to separate excitation and emission, scanning speed *etc.*, were all kept fixed during observation of the same group of experimental cells. Colocalization analysis was carried out by LSM software (version 3.0). Line scan analysis was also performed by the software. Fluorescent intensity numerals of each line scan were exported to MS Excel, the mean $\pm$ SD as well as HI values of intensity value for segment of interest were calculated. MS Excel also constructed the line scan fluorescent intensity fluctuation graphs of the representative cells. All images obtained represent the average of eight sequentially obtained images. LSM images were exported as TIF files, and final figures were generated using Adobe Illustrator and Adobe Photoshop (Adobe Systems, Inc., San Jose, CA).

Fluorescence recovery after photobleaching (FRAP) analysis were also carried out by the LSM 510 META confocal microscope. A single Z section was imaged before and at time intervals after a 2-sec bleach. The bleach was carried

out at a wavelength of 514 nm and maximum power for 50 iterations of a box representing 20% of the nuclear volume. A time-interval mode of Time Series was used with the time interval varied in different groups of experiments according to the mobility of the protein: 500 μsec was set for the Ad4BP/SF-1-H89 group (Fig. 8A), 2 sec was for the DAX-1-Ad4BP/SF-1-H89 group (Fig. 8B), and 600 μsec for the DAX-1-Ad4BP/SF-1-FK group (Fig. 8C). The fluorescence intensities of the region of interest were obtained using LSM software (version 3.0), and the data were analyzed using Microsoft Excel. The fluorescence recovery is usually incomplete, probably because attenuation of fluorescence occurs during the serial scanning and also the total amount of fluorescence protein decreases, as around 20% of them have been bleached. In addition, the fluorescent intensity after bleaching is not always the same. Therefore we normalized the raw FRAP data (both intensity of each time point and the time) by the method described by Stenoien *et al.* (51). Briefly, intensity values were normalized using the equation: $It = (Xt - Y)/(Z - Y)$, where I is the intensity at time t, X is the intensity at time t, Y is the intensity immediately after the photobleach (where t is equal to 0), and Z is the intensity at the final time point. This sets the initial postbleach intensity (at $t = 0$ sec) to 0 and the final intensity to 1 using arbitrary units. The normalized intensity values were averaged and plotted against time to make the recovery curve. The $t_{1/2}$ value can be observed from the graph as the time at which the normalized intensity reaches 0.5 arbitrary units. A subgroup of FRAPed cells was traced by initially being seeded on grid-carved glass-bottom dishes (code no. 3920-035, IWAKI, Chiba, Japan), and was subsequently subjected to quantitative immunofluorescence staining to ensure that cells selected for FRAP study also overexpressed both YFP-Ad4BP/SF-1 and pRc/RSV-DAX-1 in a reasonable range as described above.

Statistics

One-way ANOVA followed by Scheffe's test was used for multigroup comparisons.

Acknowledgments

We thank Professor Spiegelman (Department of Cell Biology, Harvard Medical School, Boston, MA) for the generous gift of the expression vector for mouse PGC-1, pcDNA-PGC-1.

Received March 28, 2003. Accepted September 30, 2003.

Address all correspondence and requests for reprints to: Toshihiko Yanase, M.D., Ph.D., Department of Medicine and Bioregulatory Science, Graduate School of Medical Science, Kyushu University, Maidashi 3-1-1, Higashi-ku, Fukuoka 812-8582, Japan. E-mail: yanase@intmed3.med.kyushu-u.ac.jp.

REFERENCES

1. Ingraham HA, Lala DS, Ikeda Y, Luo X, Shen WH, Nachtigal MW, Abbud R, Nilson JH, Parker KL 1994 The nuclear receptor steroidogenic factor 1 acts at multiple levels of the reproductive axis. Genes Dev 8:2302–2312
2. Nawata H, Yanase T, Oba K, Ichino I, Saito M, Goto K, Ikuyama S, Sakai H, Takayanagi R 1999 Human Ad4BP/SF-1 and its related nuclear receptor. J Steroid Biochem Mol Biol 69:323–328
3. Luo X, Ikeda Y, Lala DS, Baity LA, Meade JC, Parker KL 1995 A cell-specific nuclear receptor plays essential roles in adrenal and gonadal development. Endocr Res 21: 517–524
4. Morohashi KI, Omura T 1996 Ad4BP/SF-1, a transcription factor essential for the transcription of steroidogenic cytochrome P450 genes and for the establishment of the reproductive function. FASEB J 10:1569–1577
5. Parker KL, Schimmer BP 1997 Steroidogenic factor 1: a key determinant of endocrine development and function. Endocr Rev 18:361–377
6. Zhao L, Bakke M, Krimkevich Y, Cushman LJ, Parlow AF, Camper SA, Parker KL 2001 Steroidogenic factor 1 (SF1) is essential for pituitary gonadotrope function. Development 128:147–154
7. Luo X, Ikeda Y, Parker KL 1994 A cell-specific nuclear receptor is essential for adrenal and gonadal development and sexual differentiation. Cell 77:481–490
8. Achermann JC, Ito M, Ito M, Hindmarsh PC, Jameson JL 1999 A mutation in the gene encoding steroidogenic factor-1 causes XY sex reversal and adrenal failure in humans. Nat Genet 22:125–126
9. Ikeda Y, Swain A, Weber TJ, Hentges KE, Zanaria E, Lalli E, Tamai KT, Sassone-Corsi P, Lovell-Badge R, Camerino G, Parker KL 1996 Steroidogenic factor 1 and Dax-1 colocalize in multiple cell lineages: potential links in endocrine development. Mol Endocrinol 10:1261–1272
10. Swain A, Zanaria E, Hacker A, Lovell-Badge R, Camerino G 1996 Mouse Dax1 expression is consistent with a role in sex determination as well as in adrenal and hypothalamus function. Nat Genet 12:404–409
11. Crawford PA, Dorn C, Sadovsky Y, Milbrandt J 1998 Nuclear receptor DAX-1 recruits nuclear receptor corepressor N-CoR to steroidogenic factor 1. Mol Cell Biol 18:2949–2956
12. Sewer MB, Nguyen VQ, Huang CJ, Tucker PW, Kagawa N, Waterman MR 2002 Transcriptional activation of human CYP17 in H295R adrenocortical cells depends on complex formation among p54 (nrb)/NonO, protein-associated splicing factor, and SF-1, a complex that also participates in repression of transcription. Endocrinology 143:1280–1290
13. Morohashi K, Zanger UM, Honda S, Hara M, Waterman MR, Omura T 1993 Activation of CYP11A and CYP11B gene promoters by the steroidogenic cell-specific transcription factor, Ad4BP. Mol Endocrinol 7:1196–1204
14. Michael MD, Kilgore MW, Morohashi K, Simpson ER 1995 Ad4BP/SF-1 regulates cyclic AMP-induced transcription from the proximal promoter (PII) of the human aromatase P450 (CYP19) gene in the ovary. J Biol Chem 270:13561–13566
15. Ito M, Park Y, Weck J, Mayo KE, Jameson JL 2000 Synergistic activation of the inhibin α-promoter by steroidogenic factor-1 and cyclic adenosine 3′, 5′-monophosphate. Mol Endocrinol 14:66–81
16. Hager GL, Elbi C, Becker M 2002 Protein dynamics in the nuclear compartment. Curr Opin Genet Dev 12:137–141
17. Stenoien DL, Simeoni S, Sharp ZD, Mancini MA 2000 Subnuclear dynamics and transcription factor function. J Cell Biochem Suppl 35:99–106
18. Becker M, Baumann C, John S, Walker DA, Vigneron M, McNally JG, Hager GL 2002 Dynamic behavior of transcription factors on a natural promoter in living cells. EMBO Rep 3:1188–1194
19. McNally JG, Muller WG, Walker D, Wolford R, Hager GL 2000 The glucocorticoid receptor: rapid exchange with regulatory sites in living cells. Science 287:1262–1265
20. Fletcher TM, Xiao N, Mautino G, Baumann CT, Wolford R, Warren BS, Hager GL 2002 ATP-dependent mobilization of the glucocorticoid receptor during chromatin remodeling. Mol Cell Biol 22:3255–3263
21. Stenoien DL, Patel K, Mancini MG, Dutertre M, Smith CL, O'Malley BW, Mancini MA 2001 FRAP reveals that mobility of oestrogen receptor-α is ligand- and proteasome-dependent. Nat Cell Biol 3:15–23
22. Stenoien DL, Nye AC, Mancini MG, Patel K, Dutertre M, O'Malley BW, Smith CL, Belmont AS, Mancini MA 2001

Ligand-mediated assembly and real-time cellular dynamics of estrogen receptor-coactivator complexes in living cells. Mol Cell Biol 21:4404–4412
23. Maruvada P, Baumann CT, Hager GL, Yen PM 2003 Dynamic shuttling and intranuclear mobility of nuclear hormone receptors. J Biol Chem 278:12425–12432
24. Lynch JP, Lala DS, Peluso JJ, Luo W, Parker KL, White BA 1993 Steroidogenic factor 1, an orphan nuclear receptor, regulates the expression of the rat aromatase gene in gonadal tissues. Mol Endocrinol 7:776–786
25. Saitoh M, Takayanagi R, Goto K, Fukamizu A, Tomura A, Yanase T, Nawata H 2002 The presence of both the amino- and carboxyl-terminal domains in the AR is essential for the completion of a transcriptionally active form with coactivators and intranuclear compartmentalization common to the steroid hormone receptors: a three-dimensional imaging study. Mol Endocrinol 16:694–706
26. Aesoy R, Mellgren G, Morohashi K, Lund J 2002 Activation of cAMP-dependent protein kinase increases the protein level of steroidogenic factor-1. Endocrinology 143:295–303
27. Jacob AL, Lund J, Martinez P, Hedin L 2001 Acetylation of steroidogenic factor 1 protein regulates its transcriptional activity and recruits the coactivator GCN5. J Biol Chem 276:37659–37664
28. McMahon SB, Van Buskirk HA, Dugan KA, Copeland TD, Cole MD 1998 The novel ATM-related protein TRRAP is an essential cofactor for the c-Myc and E2F oncoproteins. Cell 94:363–374
29. Jacq X, Brou C, Lutz Y, Davidson I, Chambon P, Tora L 1994 Human TAFII30 is present in a distinct TFIID complex and is required for transcriptional activation by the estrogen receptor. Cell 79:107–117
30. Yanagisawa J, Kitagawa H, Yanagida M, Wada O, Ogawa S, Nakagomi M, Oishi H, Yamamoto Y, Nagasawa H, McMahon SB, Cole MD, Tora L, Takahashi N, Kato S 2002 Nuclear receptor function requires a TFTC-type histone acetyl transferase complex. Mol Cell 9:553–562
31. Ito M, Yu R, Jameson JL 1997 DAX-1 inhibits SF-1-mediated transactivation via a carboxy-terminal domain that is deleted in adrenal hypoplasia congenita. Mol Cell Biol 17:1476–1483
32. Altincicek B, Tenbaum SP, Dressel U, Thormeyer D, Renkawitz R, Baniahmad A 2000 Interaction of the corepressor Alien with DAX-1 is abrogated by mutations of DAX-1 involved in adrenal hypoplasia congenita. J Biol Chem 275:7662–7667
33. Zhang P, Mellon SH 1996 The orphan nuclear receptor steroidogenic factor-1 regulates the cyclic adenosine 3′, 5′-monophosphate-mediated transcriptional activation of rat cytochrome P450c17 (17α-hydroxylase/c17–20 lyase). Mol Endocrinol 10:147–158
34. Hammer GD, Krylova I, Zhang Y, Darimont BD, Simpson K, Weigel NL, Ingraham HA 1999 Phosphorylation of the nuclear receptor SF-1 modulates cofactor recruitment: integration of hormone signaling in reproduction and stress. Mol Cell 3:521–526
35. Carlone DL, Richards JS 1997 Functional interactions, phosphorylation, and levels of 3′, 5′-cyclic adenosine monophosphate-regulatory element binding protein and steroidogenic factor-1 mediate hormone-regulated and constitutive expression of aromatase in gonadal cells. Mol Endocrinol 11:292–304
36. Sewer MB, Waterman MR 2002 Adrenocorticotropin/cyclic adenosine 3′, 5′-monophosphate-mediated transcription of the human CYP17 gene in the adrenal cortex is dependent on phosphatase activity. Endocrinology 143:1769–1777
37. Nomura M, Kawabe K, Matsushita S, Oka S, Hatano O, Harada N, Nawata H, Morohashi K 1998 Adrenocortical and gonadal expression of the mammalian Ftz-F1 gene encoding Ad4BP/SF-1 is independent of pituitary control. J Biochem (Tokyo) 124:217–224
38. Crawford PA, Sadovsky Y, Woodson K, Lee SL, Milbrandt J 1995 Adrenocortical function and regulation of the steroid 21-hydroxylase gene in NGFI-B-deficient mice. Mol Cell Biol 15:4331–4316
39. Herzig S, Long F, Jhala US, Hedrick S, Quinn R, Bauer A, Rudolph D, Schutz G, Yoon C, Puigserver P, Spiegelman B, Montminy M 2001 CREB regulates hepatic gluconeogenesis through the coactivator PGC-1. Nature 413:179–183
40. Htun H, Barsony J, Renyi I, Gould DL, Hager GL 1996 Visualization of glucocorticoid receptor translocation and intranuclear organization in living cells with a green fluorescent protein chimera. Proc Natl Acad Sci USA 93: 4845–4850
41. Racz A, Barsony J 1999 Hormone-dependent translocation of vitamin D receptors is linked to transactivation. J Biol Chem 274:19352–19360
42. Jenster G 1999 The role of the androgen receptor in the development and progression of prostate cancer. Semin Oncol 26:407–421
43. Fejes-Toth G, Pearce D, Naray-Fejes-Toth A 1998 Subcellular localization of mineralocorticoid receptors in living cells: effects of receptor agonists and antagonists. Proc Natl Acad Sci USA 95:2973–2978
44. Tomura A, Goto K, Morinaga H, Nomura M, Okabe T, Yanase T, Takayanagi R, Nawata H 2001 The subnuclear three-dimensional image analysis of androgen receptor fused to green fluorescence protein. J Biol Chem 276: 28395–28401
45. Elbi C, Misteli T, Hager GL 2002 Recruitment of dioxin receptor to active transcription sites. Mol Biol Cell 13: 2001–2015
46. Baumann CT, Ma H, Wolford R, Reyes JC, Maruvada P, Lim C, Yen PM, Stallcup MR, Hager GL 2001 The glucocorticoid receptor interacting protein 1 (GRIP1) localizes in discrete nuclear foci that associate with ND10 bodies and are enriched in components of the 26S proteasome. Mol Endocrinol 15:485–500
47. Nishi Y, Yanase T, Mu Y, Oba K, Ichino I, Saito M, Nomura M, Mukasa C, Okabe T, Goto K, Takayanagi R, Kashimura Y, Haji M, Nawata H 2001 Establishment and characterization of a steroidogenic human granulosa-like tumor cell line, KGN, that expresses functional follicle-stimulating hormone receptor. Endocrinology 142:437–445
48. Nishi Y, Yanase T, Oba K, Ikuyama S, Takayanagi R, Nawata H 1998 Establishment and function analysis of a steroidogenic human granulosa-like tumor cell line, KGN. Clin Endocrinol (Tokyo) 46:156–161
49. Oba K, Yanase T, Ichino I, Goto K, Takayanagi R, Nawata H 2000 Transcriptional regulation of the human FTZ-F1 gene encoding Ad4BP/SF-1. J Biochem (Tokyo) 128: 517–528
50. Mu YM, Yanase T, Nishi Y, Takayanagi R, Goto K, Nawata H 2001 Combined treatment with specific ligands for PPARγ:RXR nuclear receptor system markedly inhibits the expression of cytochrome P450arom in human granulosa cancer cells. Mol Cell Endocrinol 181:239–248
51. Stenoien DL, Mielke M, Mancini MA 2002 Intranuclear ataxin1 inclusions contain both fast- and slow-exchanging components. Nat Cell Biol 4:806–810

***Molecular Endocrinology* is published monthly by The Endocrine Society (http://www.endo-society.org), the foremost professional society serving the endocrine community.**

Mitochondrial Nucleoid and Transcription Factor A

TOMOTAKE KANKI,[a] HIROSHI NAKAYAMA,[b] NARIE SASAKI,[c] KOJI TAKIO,[b] TANFIS ISTIAQ ALAM,[a] NAOTAKA HAMASAKI,[a] AND DONGCHON KANG[a]

[a]*Department of Clinical Chemistry and Laboratory Medicine, Kyushu University Graduate School of Medical Sciences, Fukuoka 812-8582, Japan*

[b]*Biomolecular Characterization Division, RIKEN (The Institute for Physical and Chemical Research), Wako 351-0198, Japan*

[c]*Department of Biology, Faculty of Science, Ochanomizu University, Tokyo 112-8610, Japan*

ABSTRACT: Nuclear DNA is tightly packed into nucleosomal structure. In contrast, human mitochondrial DNA (mtDNA) had long been believed to be rather naked because mitochondria lack histone. Mitochondrial transcription factor A (TFAM), a member of a high mobility group (HMG) protein family and a first-identified mitochondrial transcription factor, is essential for maintenance of mitochondrial DNA. Abf2, a yeast counterpart of human TFAM, is abundant enough to cover the whole region of mtDNA and to play a histone-like role in mitochondria. Human TFAM is indeed as abundant as Abf2, suggesting that TFAM also has a histone-like architectural role for maintenance of mtDNA. When human mitochondria are solubilized with non-ionic detergent Nonidet-P40 and then separated into soluble and particulate fractions, most TFAM is recovered from the particulate fraction together with mtDNA, suggesting that human mtDNA forms a nucleoid structure. TFAM is tightly associated with mtDNA as a main component of the nucleoid.

KEYWORDS: mitochondria; mitochondrial DNA; nucleoid; TFAM; transcription; HMG

INTRODUCTION

Maintenance of mitochondrial DNA (mtDNA) integrity is essential for normal function of the respiratory chain responsible for aerobic ATP production. This is clearly exemplified by many patients with encephalomyopathies caused by mtDNA mutations. mtDNA is subject to damage in part because it is under stronger oxidative stress than is nuclear DNA.[1] Naturally, mitochondria are equipped with systems for protecting their own genome.[1] Recently, the role of mitochondrial transcription factor A (TFAM) in the mtDNA-maintaining systems has gained increasing interest.

Address for correspondence: Dongchon Kang, Department of Clinical Chemistry and Laboratory Medicine, Kyushu University Graduate School of Medical Sciences, 3-1-1 Maidashi, Higashi-ku, Fukuoka 812-8582, Japan. Voice: +81-92-642-5749; fax: +81-92-642-5772.
kang@mailserver.med.kyushu-u.ac.jp

Ann. N.Y. Acad. Sci. 1011: 61–68 (2004).
doi: 10.1196/annals.1293.007

TFAM was purified and cloned as a transcription factor for mtDNA.[2,3] TFAM indeed enhances mtDNA transcription in a promoter-specific fashion in the presence of mitochondrial RNA polymerase and transcription factor B.[4] Because replication of mammalian mtDNA is to be initiated following the transcription,[5] TFAM is also thought to be crucial for replication of mtDNA. Consistent with this notion, targeted disruption of the mouse TFAM gene is an embryonic lethal mutation causing mtDNA depletion.[6] However, TFAM is virtually a DNA-binding protein with no sequence specificity, although it shows a relatively higher affinity to the light and heavy strand promoters, LSP and HSP, respectively.[2,3] TFAM is a member of the high mobility group (HMG) proteins and contains two HMG-boxes. Many HMG-family proteins bind, wrap, bend, and unwind DNA regardless of DNA sequence.[7–9] Abf2, a TFAM homologue of *Saccharomyces cerevisiae*, is also an HMG-family protein. Abf2 is abundant in yeast mitochondria: roughly one molecule to every 15 bp of mtDNA.[10] Unlike mammalian TFAM, Abf2 is not essential for either transcription initiation of mtDNA or mtDNA replication.[10] *Saccharomyces cerevisiae* devoid of Abf2 loses mtDNA when cultured in the presence of fermentable carbon sources,[11] but this mtDNA depletion is rescued by a bacterial histone-like protein HU,[12] suggesting that Abf2 maintains mtDNA as an architectural factor. Because TFAM can substitute for Abf2 as well,[3] human TFAM at least potentially retains common properties to Abf2 and HU. In this article, we show that human mtDNA is tightly associated and wrapped with TFAM, and is thus far from naked, although it is still widely believed to be naked. We propose that TFAM functions not only as a transcription factor but also as a main constitutive factor of an mtDNA/protein complex.

TFAM IN MITOCHONDRIAL NUCLEOID

mtDNA is postulated to have a nucleosome-like structure, i.e., nucleoid, in lower eukaryotes such as *Saccharomyces cerevisiae*[13] and *Physarum polycephalum*.[14] However, its structure is poorly elucidated at a molecular level. Human mtDNA was also proposed to take on a nucleoid structure, mainly based on a dotted pattern of mtDNA staining.[15,16] The human mtDNA nucleoid has not been isolated until recently[17,18] and its structure is still poorly characterized. We have found that human TFAM is two orders of magnitude more abundant than previously considered.[19] Its amount is quite comparable to that of yeast Abf2. Assuming that most TFAM molecules are bound to mtDNA, the amount of TFAM is sufficient for covering the entire length of mtDNA. The issue is whether this assumption is a fact. When human mitochondria are solubilized with a non-ionic detergent Nonidet-P40 (NP-40), most TFAM is recovered from a particulate fraction along with mtDNA,[18] indicating that few free TFAM molecules exist in mitochondria. In the NP-40–insoluble fraction (P2 fraction) of mitochondria of a human cell line of Jurkat, the TFAM/mtDNA ratio is about 900. These results suggest that about 900 molecules of TFAM are bound to one molecule of mtDNA on average. This amount of TFAM could cover the mtDNA entirely. Hence, we can no longer say that human mtDNA is naked. LSP and HSP are promoters for transcription of the light and heavy strands, respectively.[20] TFAM would bind first and leave last these two promoters, because TFAM has a higher af-

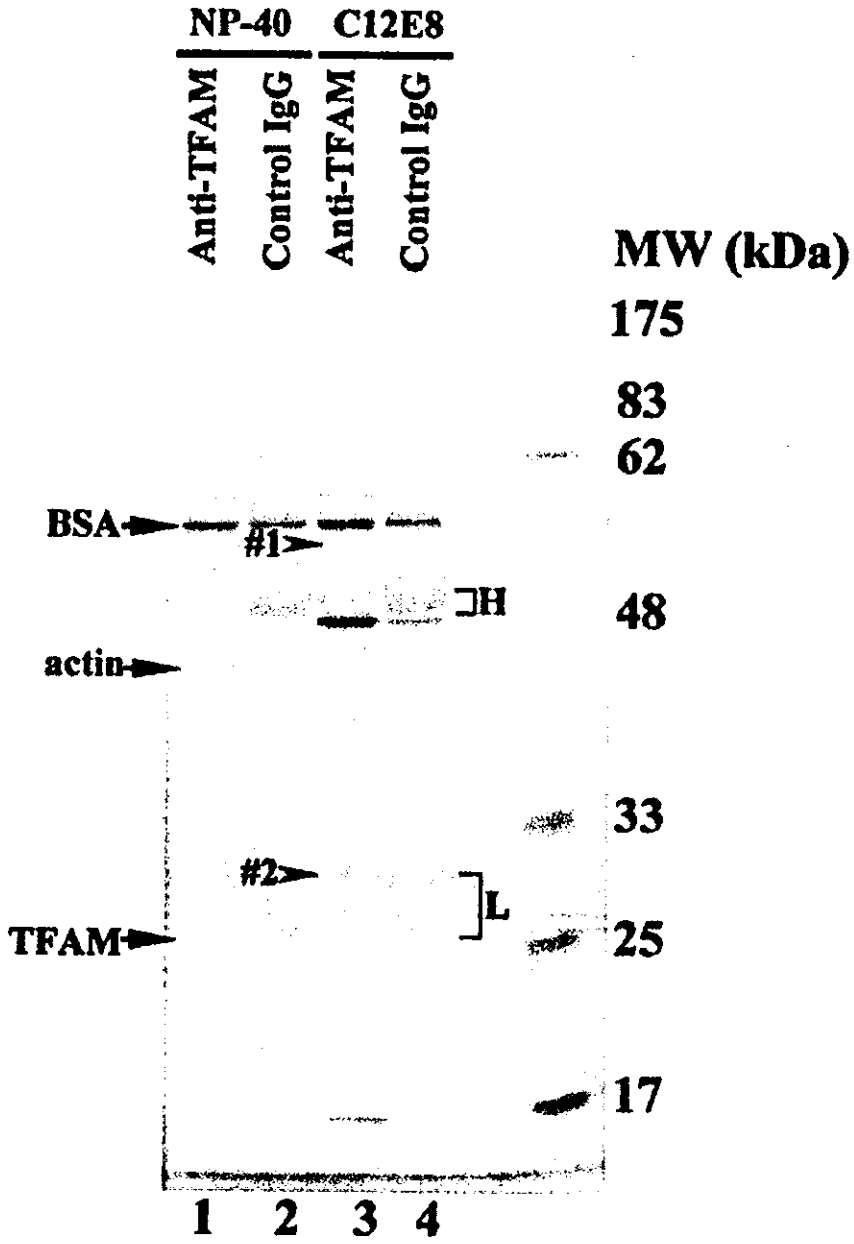

FIGURE 1. Analysis of immunoprecipitated proteins. Mitochondria were solubilized with 0.5% NP-40 or C12E8. The proteins immunoprecipitated by anti-TFAM were resolved on SDS-PAGE. Each band was excised and analyzed by mass spectrometry after lysyl endopeptidase digestion. BSA, which was used for blocking the beads, was released from the beads. #1, monoamine oxidase; #2, adenine nucleotide translocator 2; H, IgG heavy chain; L, IgG light chain.

finity for these two regions than for the rest of the mtDNA molecule.[3,21,22] Therefore, under conditions where about 900 molecules of TFAM are bound to mtDNA, LSP and HSP are likely to be persistently occupied by TFAM. Given that binding of TFAM to LSP or HSP is required to initiate transcription of mtDNA, TFAM itself would be abundant enough to constitutively and fully activate the mtDNA transcription in a normal state. Consistent with this, the gene expression of mtDNA largely depends on its copy number.[23] Thus TFAM may be essential for transcription initiation, but it seems unlikely that the transcription rate is regulated by the amount of TFAM. This idea is compatible with a recent finding that TFAM levels can be substantially reduced without significant inhibition of mtDNA transcription in insect cells.[24] In addition, TFAM alone is not able to initiate transcription from the specific promoters with purified recombinant RNA polymerase.[25,26] Recently, the human homologue of yeast mitochondrial transcription factor B has been cloned[27] and shown to be required for the promoter-specific transcription by the RNA polymerase.[17]

ASSOCIATION OF mtDNA WITH MEMBRANES

It has been proposed that human mtDNA associates with the mitochondrial inner membrane.[28] When we solubilized mitochondria with octaethylene glycol monododecyl ether (C12E8), a weaker non-ionic detergent than NP-40, more monoamine oxidase and ATP/ADP translocator, abundant outer and inner membrane proteins, respectively, were co-immunoprecipitated by anti-TFAM (FIG. 1), a result

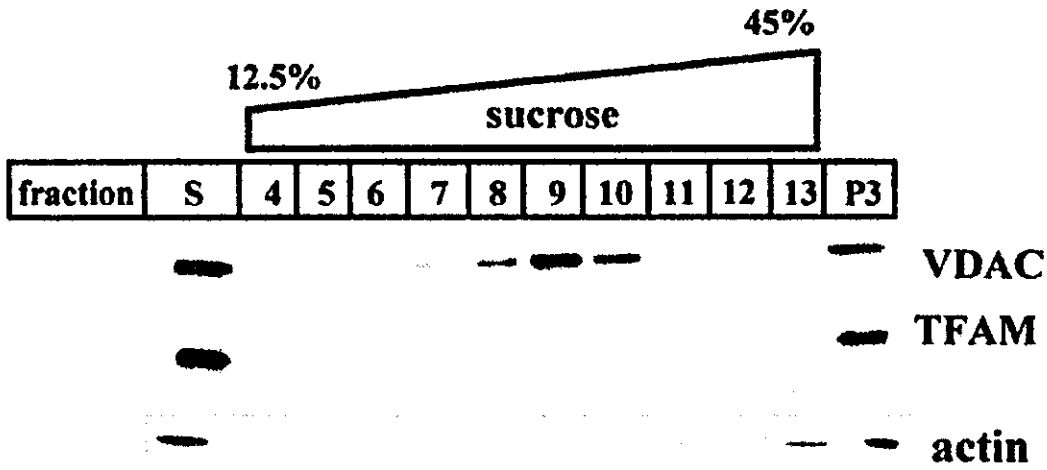

FIGURE 2. Separation of an NP-40–insoluble particulate fraction by sucrose-density gradient centrifugation. An NP-40–insoluble particulate fraction (P2) was mixed with an equal volume of buffer TEN (10 mM Tris-HCl, pH 7.0, 1 mM EDTA, and 150 mM NaCl) containing 80% sucrose (w/vol) and placed at the tube bottom. Then, stepwise sucrose gradients (5–30% in TEN buffer, 1 mL each) were layered on top. The gradient steps were serially reduced by 2.5% from the bottom to top. The tube was centrifuged at 200,000 × *g* for 15 h at 4°C. After centrifugation, 1-mL samples were collected from the top down. The pellet at the bottom was designated P3. Each fraction was collected from the top down and analyzed by Western blotting. S, starting sample; P3, pellet at the bottom.

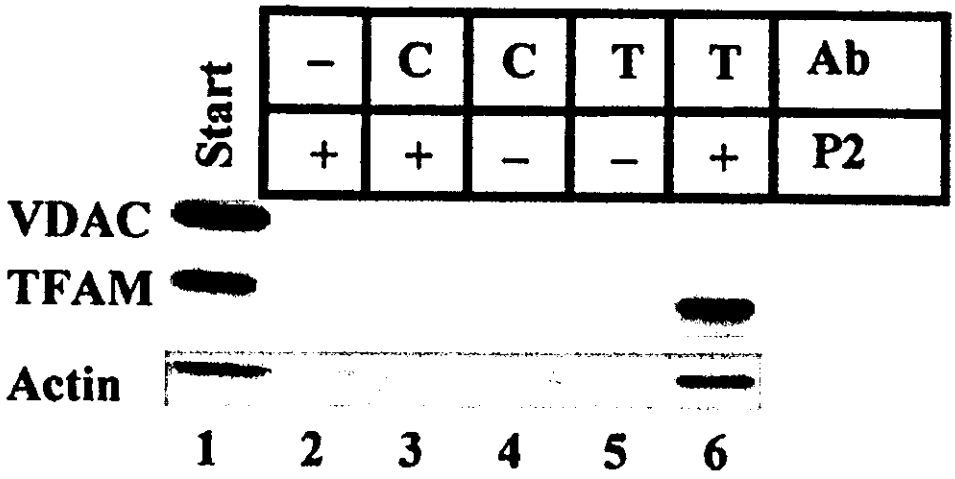

FIGURE 3. Immunoprecipitation by anti-TFAM. An NP-40–insoluble particulate fraction was incubated with rotation in the presence of antibody-immobilized magnetic beads. The beads were pelleted using a magnet. The resulting supernatants were removed. After washing three times, proteins were eluted from the beads by heating. VDAC, TFAM, and actin were detected by Western blotting. –, unconjugated magnetic beads; C, control IgG; T, anti-TFAM; VDAC, voltage-dependent anion channel.

compatible with the association of a TFAM/mtDNA complex with the membranes. It is assumed that nuclear DNA is looped into domains by attachment to some underlying skeleton (e.g., a matrix or scaffold[29]). Compared to nuclear DNA, however, little is known about how mtDNA associates with membranes. Plasma membranes harbor a special domain, a so-called raft, that is insoluble with TritonX-100. The typical rafts are recovered from around 20% sucrose fractions by sucrose-density centrifugation.[30] It is unlikely that TFAM is localized in a similar special membrane domain of mitochondria because TFAM was recovered from the bottom of the sucrose gradient (FIG. 2, fraction P3).

Our mitochondrial preparation contained actin, a major component of the cytoskeleton. The cytoskeleton is resistant to cold solubilization with non-ionic detergents, and the NP-40 insoluble fractions of the mitochondria indeed retained actin (FIG. 2, fraction S). The insoluble cytoskeleton is recovered from the bottom of the sucrose gradient,[30] and we detected actin in the bottom fraction (FIG. 2, fraction P3). Furthermore, actin was co-immunoprecipitated along with mtDNA and TFAM (FIG. 3). Actin is known to associate with mitochondria in yeast.[31] Recently it was reported that tubulin, a component of microtubules, is attached to human mitochondria.[32] It may be safe to assume that actin also associates with human mitochondrial membranes. There is a surprising report that vimentin, an intermediate filament protein, is directly cross-linked to mtDNA in mouse and human cells.[33] Intermediate filaments are interconnected to microfilaments and microtubules.[34] Taken together, it seems an attractive hypothesis that mtDNA is anchored to membranes via cytoskeletal components irrespective of whether its putative cytoskeletal association is indirect or direct. Such attachment would provide mtDNA a scaffold for transcription, replication, and repair, as in the case of nuclear DNA. Elucidation of such a relationship could also give new insights into the segregation of mtDNA.

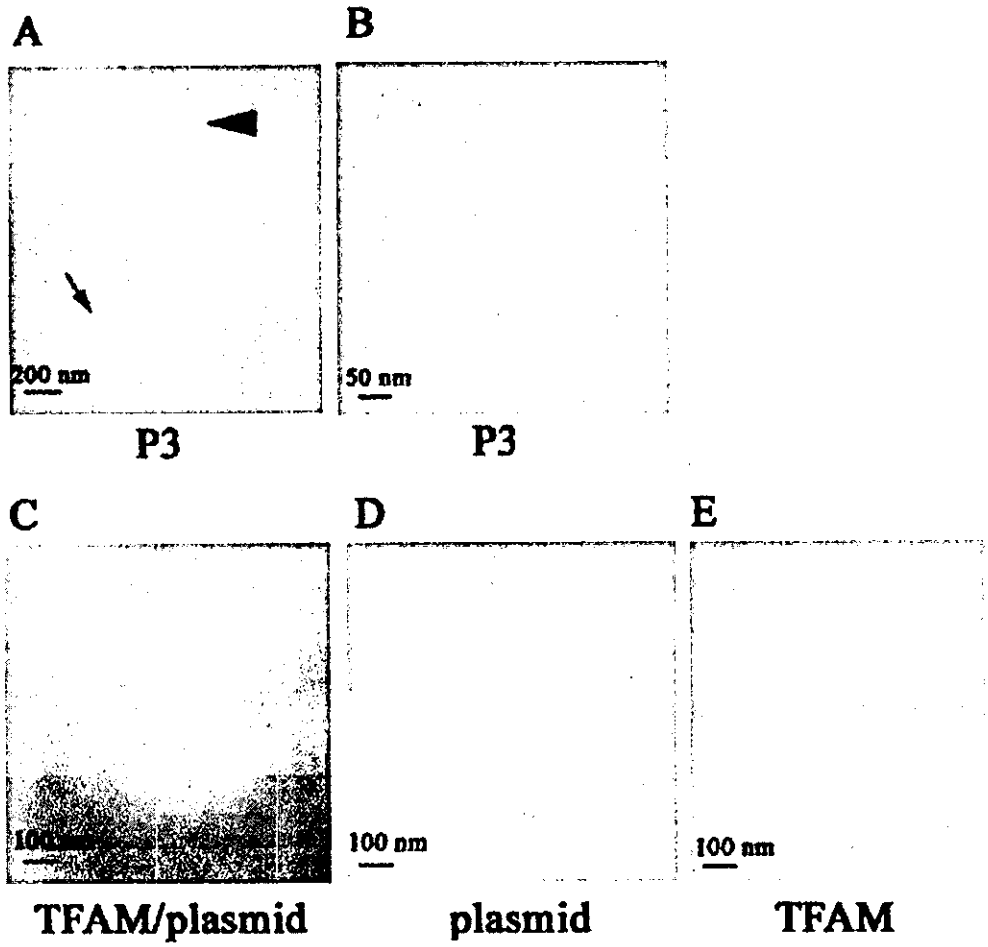

FIGURE 4. Electron microscopic structures. Four nM circular plasmids (pGL-MHC-SvpA, 9.2 kb)[35] and 2 μM recombinant human TFAM (TFAM/plasmid=500) were incubated for 10 min at 25°C in buffer containing 10 mM HEPES-NaOH, pH 7.4, 1 mM EDTA, and 150 mM NaCl. Carbon-coated grid was rendered hydrophilic by glow-discharge at low pressure in air. Samples were adsorbed to the carbon-coated grid for 1 min, and immediately stained with 1% uranyl acetate. The samples were observed in a JEOL JEM 2000 EX electron microscope operated 100 kV acceleration voltage and 60,000× magnification. (**A**) The P3 fraction was observed by electron microscopy. A typical vesicle is indicated by an arrowhead. An arrow indicates a string-like structure. (**B**) A more magnified image of a string-like structure in another area. TFAM/plasmid complexes (**C**), plasmid alone (**D**), and TFAM alone (**E**) were similarly observed by electron microscopy.

DNA WRAPPING WITH TFAM

We examined the P3 fraction by electron microscopy. Vesicle-like bodies were mainly observed in the P3 fraction (FIG. 4A, arrowhead). We also observed some bodies in which a string-like structure could be noticed (FIG. 4A, arrow, and 4B). Some mtDNA nucleoids might be exposed by removal of membrane lipids in the P3. These observations suggest that mtDNA is precipitated along with mitochondrial membranes which were not solubilized with NP-40. When we incubated circular plasmids with TFAM, we found a rosary-like structure (FIG. 4C). In the case of plasmids alone, we observed fine threads only (FIG. 4D). TFAM alone showed few structural elements (FIG. 4E). Hence, the rosary-like structure may reflect a TFAM-

plasmid complex, suggesting that TFAM in fact has the ability to cover and wrap the entire region of closed circular DNA.

CONCLUDING REMARKS

Human mtDNA has been postulated to take on a nucleoid structure, mostly on the basis of morphological observations that mtDNA stains in a punctate pattern in cells.[15,16] Our results have provided the first biochemically substantial bases for this contention. We propose that naked mtDNA is unstable and that formation of the mtDNA nucleoid structure is one of the major functions of TFAM for maintaining mtDNA, based on the following evidence provided by several groups including ours: (1) TFAM indeed can wrap circular plasmids entirely (FIG. 4); (2) TFAM is able to substitute for Abf2, a TFAM homologue of yeast, which is supposed to mainly play a histone-like role for maintaining mtDNA;[3] (3) TFAM is abundant enough to cover mtDNA;[19] (4) most mtDNA molecules are associated with TFAM;[18] (5) most TFAM is associated with mtDNA;[18] and (6) the 50% reduction in TFAM in *TFAM*$^{+/-}$ mice decreases mtDNA by roughly 50%.[6]

ACKNOWLEDGMENTS

This work was supported in part by Uehara Memorial Foundation and Grants-in-Aid for Scientific Research from the Ministry of Education, Science, Technology, Sports, and Culture of Japan.

REFERENCES

1. KANG, D. & N. HAMASAKI. 2002. Maintenance of mitochondrial DNA integrity: repair and degradation. Curr. Genet. **41:** 311–322.
2. FISHER, R.P. & D.A. CLAYTON. 1988. Purification and characterization of human mitochondrial transcription factor 1. Mol. Cell. Biol. **8:** 3496–3509.
3. PARISI, M.A. *et al.* 1993. A human mitochondrial transcription activator can functionally replace a yeast mitochondrial HMG-box protein both *in vivo* and *in vitro*. Mol. Cell. Biol. **13:** 1951–1961.
4. FALKENBERG, M. *et al.* 2002. Mitochondrial transcription factors B1 and B2 activate transcription of human mtDNA. Nat. Genet. **31:** 289–294.
5. SHADEL, G.S. & D.A. CLAYTON. 1997. Mitochondrial DNA maintenance in vertebrates. Annu. Rev. Biochem. **66:** 409–435.
6. LARSSON, N.G. *et al.* 1998. Mitochondrial transcription factor A is necessary for mtDNA maintenance and embryogenesis in mice. Nat. Genet. **18:** 231–236.
7. BUSTIN, M. 1999. Regulation of DNA-dependent activities by the functional motifs of the high-mobility-group chromosomal proteins. Mol. Cell. Biol. **19:** 5237–5246.
8. WOLFFE, A.P. 1994. Architectural transcription factors. Science **264:** 1100–1103.
9. WOLFFE, A.P. 1999. Architectural regulations and HMG1. Nat. Genet. **22:** 215–217.
10. DIFFLEY, J.F.X. & B. STILLMAN. 1992. DNA binding properties of an HMG1-related protein from yeast mitochondria. J. Biol. Chem. **267:** 3368–3374.
11. DIFFLEY, J.F.X. & B. STILLMAN. 1991. A close relative of the nuclear, chromosomal high-mobility group protein HMG1 in yeast mitochondria. Proc. Natl. Acad. Sci. USA **88:** 7864–7868.

12. MEGRAW, T.L. & C.B. CHAE. 1993. Functional complementarity between the HMG-like yeast mitochondrial histone HM and bacterial histone-like protein HU. J. Biol. Chem. **268:** 12758–12763.
13. MIYAKAWA, I. *et al.* 1987. Isolation of morphologically intact mitochondrial nucleoids from the yeast, *Saccharomyces cerevisiae*. J. Cell Sci. **88:** 431–439.
14. SASAKI, N. *et al.* 1998. DNA synthesis in isolated mitochondrial nucleoids from plasmodia of *Physarum polycephalum*. Protoplasma **203:** 221–231.
15. SATOH, M. & T. KUROIWA. 1991. Organization of multiple nucleoids and DNA molecules in mitochondria of a human cell. Exp. Cell Res. **196:** 137–140.
16. SPELBRINK, J.N. *et al.* 2001 Human mitochondrial DNA deletions associated with mutations in the gene encoding Twinkle, a phage T7 gene 4-like protein localized in mitochondria. Nat. Genet. **28:** 223–231.
17. GARRIDO, N. *et al.* 2003. Composition and dynamics of human mitochondrial nucleoids. Mol. Biol. Cell. **14:** 1583–1596.
18. ALAM, T.I. *et al.* 2003. Human mitochondrial DNA is packaged with TFAM. Nucleic Acids Res. **31:** 1640–1645.
19. TAKAMATSU, C. *et al.* 2002. Regulation of mitochondrial D-loops by transcription factor A and single-stranded DNA-binding protein. EMBO Rep. **3:** 451–456.
20. CLAYTON, D.A. 1991. Replication and transcription of vertebrate mitochondrial DNA. Annu. Rev. Cell Biol. **7:** 453–478.
21. FISHER, R.P. *et al.* 1991. A rapid, efficient method for purifying DNA-binding proteins. J. Biol. Chem. **266:** 9153–9160.
22. OHNO, T. *et al.* 2000. Binding of human mitochondrial transcription factor A, an HMG box protein, to a four-way DNA junction. Biochem. Biophys. Res. Commun. **271:** 492–498.
23. WILLIAMS, R.S. 1986. Mitochondrial gene expression in mammalian striated muscle. J. Biol. Chem. **261:** 12390–12394.
24. GOTO, A. *et al.* 2001. *Drosophila* mitochondrial transcription factor A (d-TFAM) is dispensable for the transcription of mitochondrial DNA in Kc167 cells. Biochem. J. **354:** 243–248.
25. NAM, S.C. & C. KANG. 2001. Expression of cloned cDNA for the human mitochondrial RNA polymerase in *Escherichia coli* and purification. Protein Expr. Purif. **21:** 485–491.
26. PRIETO-MARTIN, A. *et al.* 2001 A study on the human mitochondrial RNA polymerase activity points to existence of a transcription factor B-like protein. FEBS Lett. **503:** 51–55.
27. MCCULLOCH, V. *et al.* 2002. A human mitochondrial transcription factor is related to RNA adenine methyltransferases and binds S-adenosylmethionine. Mol. Cell. Biol. **22:** 1116–1125.
28. JACKSON, D.A. *et al.* 1996. Sequences attaching loops of nuclear and mitochondrial DNA to underlying structures in human cells: the role of transcription units. Nucleic Acids Res. **24:** 1212–1219.
29. GETZENBERG, R.H. *et al.* 1991. Nuclear structure and the three-dimensional organization of DNA. J. Cell. Biochem. **47:** 289–299.
30. BROWN, D.A. & J.K. ROSE. 1992 Sorting of GPI-anchored proteins to glycolipid-enriched membrane subdomains during transport to the apical cell surface. Cell **68:** 533–544.
31. YAFFE, M.P. 1999. The machinery of mitochondrial inheritance and behavior. Science **283:** 1493–1497.
32. CARRE, M. *et al.* 2002. Tubulin is an inherent component of mitochondrial membranes that interacts with the voltage-dependent anion channel. J. Biol. Chem. **277:** 33664–33669.
33. TOLSTONOG, G.V. *et al.* 2001. Isolation of SDS-stable complexes of the intermediate filament protein vimentin with repetitive, mobile, nuclear matrix attachment region, and mitochondrial DNA sequence elements from cultured mouse and human fibroblasts. DNA Cell Biol. **20:** 531–554.
34. HERRMANN, H. & U. AEBI. 2000. Intermediate filaments and their associates: multi-talented structural elements specifying cytoarchitecture and cytodynamics. Curr. Opin. Cell. Biol. **12:** 79–90.
35. KUBOTA, T. *et al.* 1997. Cardiac-specific overexpression of tumor necrosis factor-alpha causes lethal myocarditis in transgenic mice. J. Card. Fail. **3:** 117–124.

J. Biochem. 136, 97–106 (2004)
DOI: 10.1093/jb/mvh100

Massspectrometric Analyses of Transmembrane Proteins in Human Erythrocyte Membrane

Yoshito Abe, Tomohito Chaen, Xiu Ri Jin, Tomohiro Hamasaki and Naotaka Hamasaki*

Department of Clinical Chemistry and Laboratory Medicine, Graduate School of Medical Sciences, Kyushu University, Fukuoka 812-8582, Japan

Received March 30, 2004; accepted May 6, 2004

It is difficult to understand the functional mechanisms of integral membrane proteins without having protein chemical information on these proteins. Although there have been many attempts to identify functionally important amino acids in membrane proteins, chemically and enzymatically cleaved peptides of integral membrane proteins have been difficult to handle because of their hydrophobic properties. In the present study, we have applied an analytical method to transmembrane proteins combining amino acid sequencing, matrix-assisted laser desorption ionization-time of flight (MALDI-TOF) mass spectrometry, and liquid chromatography with electrospray ionization (LC/ESI) mass spectrometry. We could analyze most (97%) of the tryptic fragments of the transmembrane domains of band 3 as well as other minor membrane proteins. The peptide mapping of the transmembrane domain of band 3 was completed and the peptide mapping information allowed us to identify the fragments containing lysine residues susceptible to 4-acetamido-4′-isothiocyanatostilbene-2,2′-disulfonic acid (SITS) and to 2,4-dinitrofluorobenzene (DNFB). This method should be applicable to membrane proteins not only in erythrocyte membranes but also in other membranes.

Key words: LC/ESI mass spectrometry, MALDI-TOF mass spectrometry, membrane protein, peptide mapping, transmembrane.

Abbreviations: BSA, bovine serum albumin; CNBr, cyanogen bromide; $C_{12}E_8$, octaethylene glycol monododecyl ether; DIDS, 4,4′-diisothiocyanostilbene-2,2′-disulfonic acid; DNDS, 4,4′-dinitrostilbene-2,2′-disulfonic acid; DNFB, 2,4-dinitrofluorobenzene; DNP, 2,4-dinitrophenyl; H_2DIDS, 4,4′-diisothiocyanodihydrostilbene-2,2′-disulfonic acid; LC/ESI, liquid chromatography with electrospray ionization; MALDI-TOF, matrix-assisted laser desorption/ionization-time of flight; PTH, phenylthiohydantoin; RP-HPLC, reverse phase-high performance liquid chromatography; SITS, 4-acetamido-4′-isothiocyanatostilbene-2,2′-disulfonic acid; TFA, trifluoroacetic acid; TM, transmembrane spanning portion; TPCK, L-(1-tosylamido-2-phenyl)ethyl chloromethyl ketone.

Membrane proteins are integrated in the lipid bilayer and play key roles in cell viability and cell metabolism. They function as transporters and signal transmitters between intra- and extra-cellular compartments. Only a limited number of integral membrane proteins have been crystallized and analyzed by X-ray crystallography (*1–4*). Most membrane protein structures have been topologically predicted simply by hydropathy predictions based on their DNA sequences. Recent studies have indicated, however, that those hydropathy predictions are not necessarily and convincingly applicable to multi-spanning membrane proteins (*5–7*). Therefore, it is necessary to collect protein chemical information as well as tertiary structural information on membrane proteins.

In the context of the structure and function relationship, protein chemical information helps us to understand the molecular mechanisms of proteins. To identify modified amino acid residues, proteins are usually fragmented either enzymatically or chemically, and the resulting fragments analyzed. The recent development of mass spectrometric techniques has enabled the rapid and sensitive identification of fragmented peptides at the pmol to fmol level. In the case of membrane proteins, however, especially multi-spanning integral membrane proteins, it is difficult to determine modified residues because of the difficulty in analyzing transmembrane peptides. Since these peptides are buried in the membrane, they are not easily accessible to proteinases. The hydrophobic properties of transmembrane segments result in their aggregation during enzymatically and chemically-mediated cleavage and high performance liquid chromatography (HPLC) separation. In a recent proteome project, the treatment of hydrophobic peptides was problematic for protein identification (*8, 9*). Therefore, hydrophobic transmembrane peptide treatment methods need to be established.

Band 3 is a typical multi-spanning integral membrane protein in erythrocytes that exchanges chloride and bicarbonate ions between the intra and extracellular side. It comprises two structurally and functionally distinct domains (*10–12*). The 40-kDa NH_2-terminal domain is located in the cytosol and interacts with the cytoskeleton. The COOH-terminal 55-kDa domain is integrated into the membrane lipid bilayer with 14 spanning transmembrane segments assumed by hydropathy predictions

*To whom correspondence should be addressed: Naotaka Hamasaki, Tel: +81-92-642-5748, Fax: +81-92-642-5772, E-mail: hamasaki@cclm.med.kyushu-u.ac.jp

(*13*), and is both necessary and sufficient for anion transport function after proteolytic removal of the cytosolic 40-kDa domain (*14*, *15*). Studies of the function and structure of the 55-kDa transmembrane domain suggest that some arginine, lysine, glutamic acid, and histidine residues play an important role in anion transport (*16–20*). These important residues, namely Lys 539 (*21*), Lys 851 (*21*, *22*), Glu 681 (*20*) and His 834 (*23*) were identified by chemical modification and mutation studies; however, the other residues have not yet been identified, because handling the transmembrane peptides of band 3 is as difficult as in the case of other integral membrane proteins.

In the present study, we have applied a peptide analytical method to erythrocyte membrane proteins and identified all peptides originating from the 55-kDa band 3 transmembrane domains (Gly 361–Val 911) using amino acid sequencing, matrix-assisted laser desorption/ionization-time of flight (MALDI-TOF) mass spectrometry, and liquid chromatography with electrospray ionization (LC/ESI) mass spectrometry. The method allowed us to identify the lysines susceptible to chemical modifications in band 3 by various reagents. Further, we identified peptide fragments from other minor erythrocyte membrane proteins using the LC/MS/MS system. These methods are applicable to the study of transmembrane proteins in erythrocyte membranes.

MATERIALS AND METHODS

Materials—3,5-Dimethoxy-4-hydroxycinnamic acid (sinapinic acid) and α-cyano-4-hydroxycinnamic acid were purchased from Aldrich Chemicals (Milwaukee, WI). L-(1-tosylamido-2-phenyl)ethyl chloromethyl ketone (TPCK)-trypsin (sequence grade) and N-glycosidase F were purchased from Roche Diagnostics (Mannheim, Germany). Trifluoroacetic acid (TFA) and other chemical reagents were purchased from Wako Co., Ltd. (Osaka, Japan).

Preparation of Erythrocyte Membranes for Peptide Analysis—Human blood stored at 4°C in acid/citrate/dextrose solution was obtained from the Fukuoka Red Cross Center. Erythrocytes were stored for less than 2 wk. Erythrocyte membranes (white ghosts) were prepared as described previously (*24*). The membranes (containing 1 mg of protein) were treated with *N*-glycosidase F (2 U) in 200 μl of 20 mM phosphate buffer (pH 7.2) for 24 h at room temperature. To remove the NH_2-teminal 40-kDa domain of band 3, membranes were pretreated with a low concentration of TPCK-trypsin (1 μg/ml) in 5 mM $NaHCO_3$ on ice for 30 min. Peripheral membrane proteins and peptides on erythrocyte membranes were removed with 10 mM NaOH. The membranes were then washed three times with 5 mM $NaHCO_3$.

Preparation of Tryptic Peptide Fragments of Erythrocyte Membrane Proteins—Tryptic peptide fragments for analyses were prepared as follows. The pretreated membranes were solubilized in a total volume of 200 μl of 0.1 M Tris-HCl (pH 8) buffer containing 0.1% $C_{12}E_8$ (octaethylene glycol monododecyl ether). The proteins in the solution (0.6 mg/ml) were digested with 4 μg TPCK-trypsin for 2 h at 37°C. The purified transmembrane domain of band 3 in 0.1% $C_{12}E_8$ solution was prepared according to Casey *et al.* (*25*), and digested with TPCK-trypsin under the same conditions.

Preparation of Modified Membranes with 4-Acetamido-4'-isothiocyanatostilbene-2,2'-disulfonic Acid (SITS) and 2,4-Dinitrofluorobenzene (DNFB)—Membranes were modified with SITS and DNFB according to previous studies (*24*, *26*). In brief, the pretreated membranes were modified with 0.1 mM SITS in 20 mM borate-buffer, pH 9.5 at 4°C for 90 min, and with 1 mM DNFB in 20 mM Tris-HCl buffer, pH 8, at 37°C for 30 min. Some membranes were preincubated with 100 μM 4,4'-dinitrostilbene-2,2'-disulfonic acid (DNDS), pH 8, at 37°C for 30 min before modification. The modified membranes were washed three times with 6 volumes of 5 mM $NaHCO_3$ containing 0.5% bovine serum albumin (BSA) and then washed three times with 5 mM $NaHCO_3$ at 4°C.

CNBr (Cyanogen Bromide) Treatment—The peptides were dissolved in 100 μl of 50% TFA solution, and incubated with 10 μg CNBr for 12 h at room temperature. After CNBr treatment, the peptides were lyophilized and stored at 4°C until analysis.

HPLC Separation of Peptide Fragments—After centrifugation (13,000 × *g* 10 min), the peptides were applied directly to an HPLC system. Samples (each 50 μl; 30 μg) were loaded onto a C_{18} reverse phase–HPLC column (RP-HPLC; cosmosil 4.6 ID × 250 mm), and eluted with a gradient of water (solvent A) and 2:1 (v/v) isopropanol/acetonitrile (solvent B), each containing 0.1% TFA, at a flow rate of 800 μl/min. The mobile phase composition was maintained at 5% B for 5 min, and then raised from 5% to 85% over 60 min and from 85 to 100% over 20 min. The eluted peptides were monitored by their absorbance at 214-nm. The SITS-modified and DNFB-modified peptides were monitored by their fluorescence at 430-nm (excitation, 340-nm) and absorbance at 340-nm, respectively. We collected the peptide fractions using the reference peaks, and the fractions were lyophilized and stored at 4°C until analysis.

Amino Acid Sequencing and Mass Spectrometry—The peptides were analyzed on a gas phase sequencer (Applied Biosystems, model 492, Foster City, CA). The phenylthiohydantions (PTHs) were identified by an Applied Biosystems 140C PTH analyzer on line system. MALDI-TOF mass spectrometric analyses were performed using a Voyager RP spectrometer (Applied Biosystems) with the acceleration voltage set to 20 kV. Data were acquired in the positive linear mode of operation, and the spectra were externally calibrated with calibration kits I and II (Applied Biosystems). The collected peptides were dissolved in 2:1 (v/v) isopropanol/acetonitrile and 0.1% TFA. The peptide solutions (0.5 μl) were mixed with 0.5 μl of matrix solutions (sinapinic acid and α-cyano-4-hydroxycinnamic acid saturated with 0.1% TFA and 50% acetonitrile in aqueous solution, respectively). The theoretical masses of each peptide were calculated using protein prospector on the World Wide Web (http://prospector.ucsf.edu/).

LC/ESI-MS was performed using a combination of HPLC (Waters 600E, Waters) and an LCQ Advantage Ion Trap Mass Spectrometer (Finnigan, San Jose, CA, USA). Each sample (10 μl; 6 μg) was loaded onto a C_{18} RP-HPLC column (2.1 ID × 250 mm;Waters Symmetry 300 C_{18} 5 mm) after centrifugation (13,000 × *g* 10 min). The peptides were separated by HPLC using a gradient of water

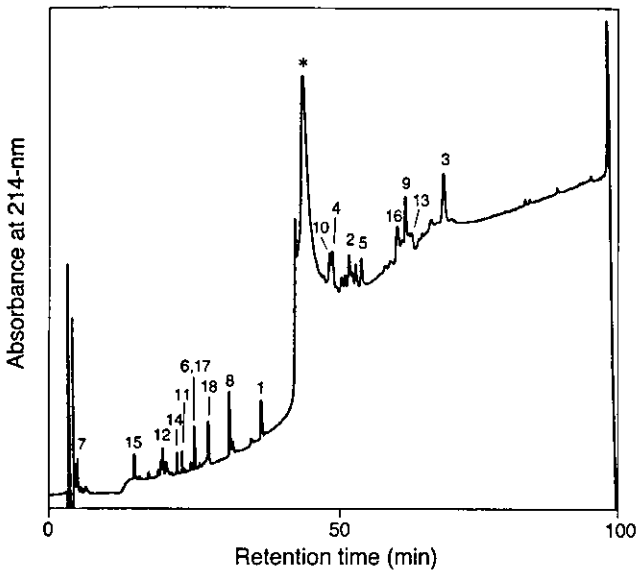

Fig. 1. **HPLC separation profile of tryptic fragments of the purified transmembrane domain of band 3 with detection at 214 nm.** The protein was dissolved in 0.1 M Tris-HCl (pH 8) buffer containing 0.1% $C_{12}E_8$, and digested with trypsin. The tryptic peptides were separated by HPLC on a reverse phase column (Cosmosil 4.6 ID × 250 mm, Nakarai, Tokyo, Japan) with a water/acetonitrile/isopropanol eluent system containing 0.1% TFA as described under "MATERIALS AND METHODS." The peak fractions from 1 to 18 were analyzed by amino acid sequencing and mass spectrometry and the results of the analyses are summarized in Table 1. The peaks indicated by asterisks contained no peptide fragments detectable by amino acid sequencing and mass spectrometry.

(solvent A) and 2:1 (v/v) isopropanol/acetonitrile (solvent B), each containing 0.025% TFA, at a flow rate of 1 ml/min. The mobile phase composition was maintained at 5% B for 5 min, and then B was increased from 5 to 85% in 60 min and from 85 to 100% in 20 min. The column eluent was split and 20% of the flow (200 μl/min) was directed into the ESI source. Data were acquired and analyzed using LCQ version 2.0 software (Finnigan, San Jose, CA). Instrument parameters were as follows: ESI needle voltage, 5 kV; ESI capillary temp, 260°C; ion energy, 35%; isolation window, 2 amu; scan range 550–2,000 amu. Peptides from the MS/MS results were identified using TURBO SEQUEST software ver. 2.0 (Finnigan, San Jose, CA) (*27*) against a human protein database extracted from the NCBI protein database. Matches to peptides identified by TURBO SEQUEST were filtered according to their cross correlation scores (X_{corr}), normalized difference in correlation scores (ΔC_n), and the tryptic nature of each peptide. The parameters used were conservative and chosen to filter the results to minimize the inclusion of false positives. All accepted results had a ΔC_n of at least 0.35 and X_{corr} of at least 2.0.

Analytical Procedures—Sodium dodecyl sulfate–polyacrylamide gel electrophoresis for protein and peptide analyses was performed according to the methods of Laemmli (*28*) and Kawano and Hamasaki (*29*). Protein concentration was determined by the method of Lowry *et al.* (*30*) using BSA as the standard.

RESULTS

HPLC Separation and Identification of Tryptic Peptides from Band 3—For analysis, the purified transmembrane domain of band 3 was dissolved in 0.1% $C_{12}E_8$ (final concentration) and digested with TPCK-trypsin. After tryptic digestion, the peptides were separated by RP-HPLC using an acetonitrile and isopropanol mixture as the solvent. We collected each peptide fraction as a reference at 214-nm absorbance (Fig. 1). The peptide fractions were analyzed for their N-terminal sequences and molec-

Table 1. **Tryptic peptide fragments of the transmembrane domain of band 3 analyzed by amino acid sequencing, MALDI-TOF mass spectrometry, and LC/ESI mass spectrometry.**

No.	Start	End	Mass calculated [MH⁺][a]	Mass observed by MALDI-TOF MS[b]	Amino acid sequencer	The most intense mass observed in LC/ESI MS	The mass from LC/ESI MS[c]
1	361	384	2,468.73	2,468.73	GLDLNGG	1,234.9 (+2)[d]	2,468.2
2	388	430	4,757.57	4,758.00	RRYPYYLS	1,586.2 (+3)	4,757.0
3	433	551	1,3504.17	1,3504.00	NQMGVSE	1,350.9 (+10)	13,503.0
4	552	600	5,546.76	5,546.78	TYNYNVL	1,387.1 (+4)	5,545.5
5	604	631	3,173.78	3,173.35	VIGDFGV	1,058.3 (+3)	3,173.0
6	632	639	863.00	861.99	LSVPDGF	862.4 (+1)	863.4
7	640	646	720.76	721.78	VSDSSAR[e]	ND[f]	ND
8	647	656	1,148.40	1,147.53	GWVIHPL	574.6 (+2)	1,148.6
9	657	694	4,354.29	4,354.36	SEFPIWM	1,451.8 (+3)	4,353.3
10	699	730	3,274.91	3,274.83	GSGFHLD	1,092.0 (+3)	3,274.6
11	731	743	1,329.56	1,328.66	SVTHANA	665.0 (+2)	1,329.4
12	744	757	1,371.53	1,370.02	ASTPGAA	686.1 (+2)	1,370.2
13	758	817	6,612.26	6,612.29	EQRISGLL	1,653.5 (+4)	6,610.9
14	818	826	1,118.28	1,118.65	YHPDVPY	559.4 (+2)	1,118.3
15	830	832	462.53	ND	TWR	ND	ND
16	833	879	5,284.75	5,284.76	MHLFTGI	1,761.8 (+3)	5,284.0
17	880	892	1,434.56	1,435.85	NVELQXL	717.5 (+2)	1,434.0
18	893	911	2,203.32	2,202.79	ATFDEEE	1,101.6 (+2)	2,202.1

[a]Calculated from average isotopic masses.[b]Mass spectrometry.[c]Calculated from the masses of multiple charge ions. [d]Most intense ions in the charge state are shown in parentheses. [e]Sugar-linked asparagine 642 changes to aspartate following digestion with N-glycosidase F. [f]Not detected.

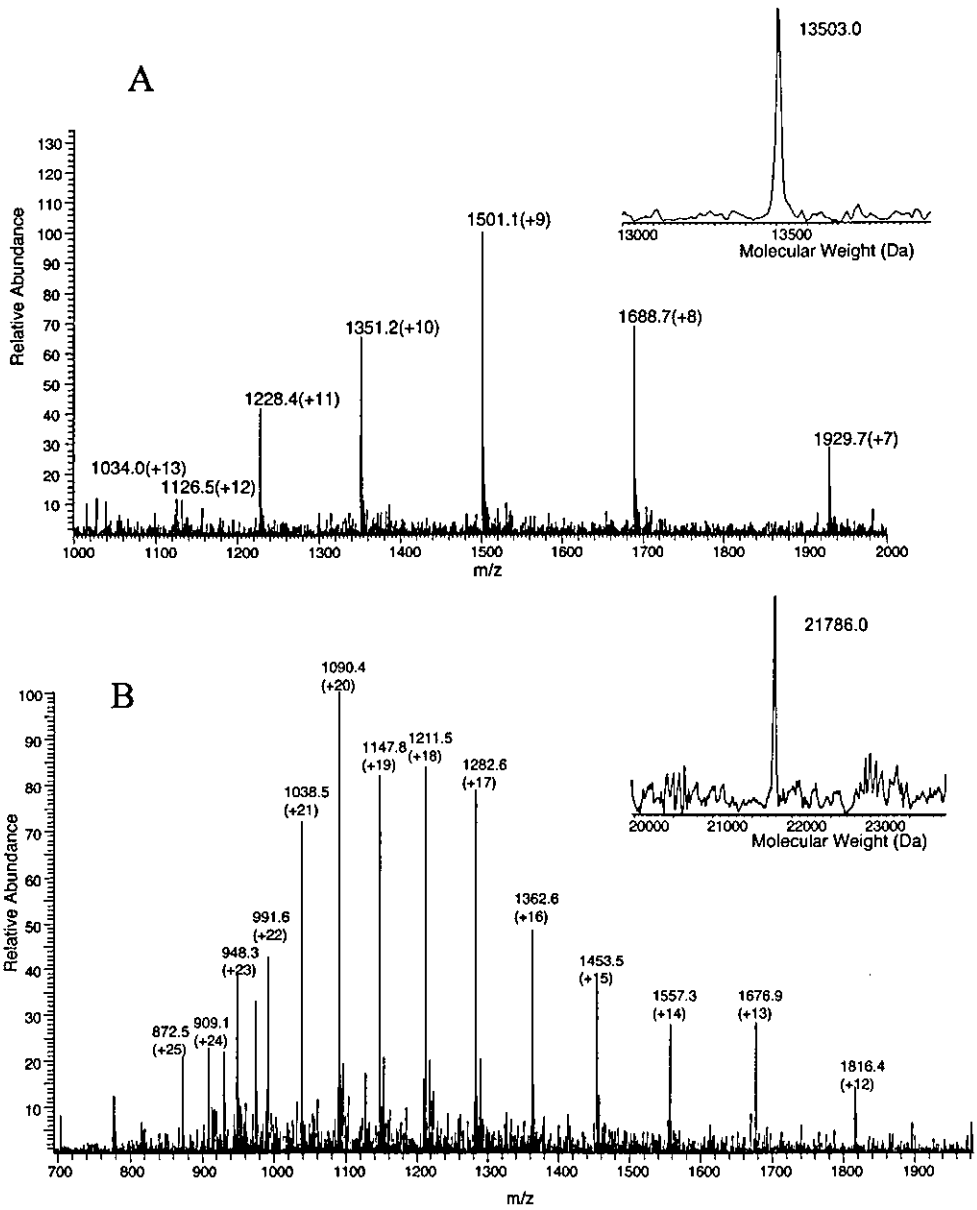

Fig. 2. The ESI mass spectra of tryptic fragment from intact membranes and SITS modified membranes. (A) The spectrum is shown for peptide fragment No.3 with ions carrying positive charges from 7 to 13. The insets show the reconstructed mass peaks for the peptide. The molecular mass, 13503, is identical to the predicted mass of tryptic fragment No. 3. (B) The spectrum is shown for the peptide fragment from SITS-modified membranes with ions carrying positive charges from 12 to 25. The inset molecular mass, 21,786, suggests that the peptide comprises Gly 361 to Lys 551 (predicted mass, 21,334) containing one SITS (molecular weight 452) molecule.

ular masses using an amino acid sequencer and MALDI-TOF mass spectrometry (Table 1). We analyzed band 3 fragment peptides by LC/ESI mass spectrometry. Mainly, peptides were determined by detection of the molecular ions derived from multiple charge states. As an example, for fragment no. 3, we could observe the masses from the multiple charged ions, 1,929.7 (+7), 1,688.7 (+8), 1,501.1 (+9), 1,351.2 (+10), 1,228.4 (+11), 1,126.5 (+12), 1,034.0 (+13) (Fig. 2A). Reconstruction of the masses from each ion indicates that the molecular weight of fragment no. 3 is 13,503 (Fig. 2A, inset). The molecular weights of other fragments were also determined (Table 1). The molecular weights determined by LC/ESI mass spectrometry were identical to the masses determined by MALDI-TOF mass spectrometry and the calculated theoretical molecular weights. Further, we could confirm the band 3 peptides using MS/MS, except for large fragments with mass greater than 5,000 kDa. Figure 3 shows the selected ion chromatograms generated by the most intense molecular ion charge state for each tryptic fragment. These peaks were well separated and well shaped, and had little tendency to aggregate. As a result, almost all tryptic peptides in the transmembrane domain were identified (Fig. 4, 97% of the sequence) except for fragments too short to be observed by this analytical method. Thus, we were able to produce a peptide map of the transmembrane domains of band 3.

Peptide Analyses of Transmembrane Proteins in Intact Human Erythrocyte Membrane—To analyze the peptides from band 3 in intact erythrocyte membranes, the membranes were solubilized in 0.1% $C_{12}E_8$ solution and digested with TPCK-trypsin. To simplify the peptide analysis, the N-terminal region (40-kDa) of band 3, *N*-linked suger and peripheral proteins were removed before membrane solubilization. The peptides were separated by RP-HPLC and analyzed by an amino acid sequencing, MALDI-TOF, and LC/ESI mass spectrometry. These fragments originating from band 3 coincided

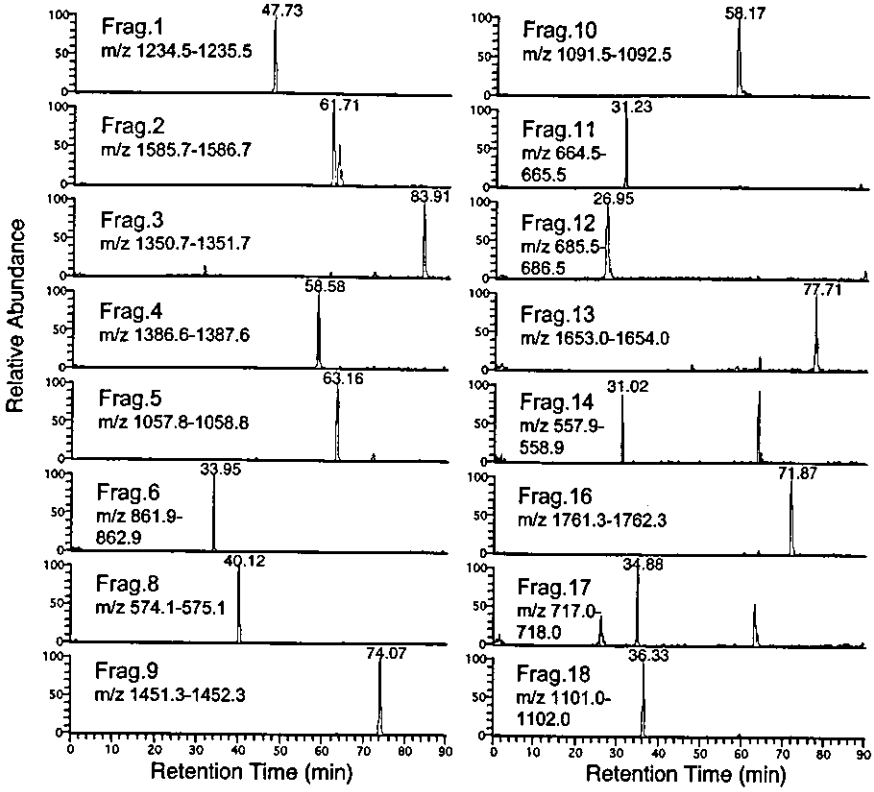

Fig. 3. **Selected ion chromatograms from ESI-MS detection of peaks from the HPLC separation of tryptic fragments of the transmembrane domain of band 3.** The protein was dissolved in 0.1 M Tris-HCl (pH 8) buffer containing 0.1% $C_{12}E_8$, and digested with trypsin. The tryptic peptides were separated by HPLC using a reversed-phase column (Waters Symmetry 300 C_{18} 5 μm, 2.1 ID × 250 mm; Waters, Milford, MA) with a water/acetonitrile/2-propanol eluant system containing 0.025% trifluoroacetic acid as described under "MATERIALS AND METHODS." Chromatograms were generated by the most intense molecular ion charge state within the mass/charge range of the instrument.

completely with the peptide fragments from the identified purified proteins (data not shown). This shows that the method can be applied to the study of the band 3 protein in intact erythrocyte membranes.

Based on the results of the analysis of intact membranes, we also could analyze peptide fragments from other erythrocyte integral membrane proteins using this analytical method. Mainly, analyses were performed using the TURBO SEQUEST program based on the MS/MS data for each peptide fragment as obtained by LC/ESI mass spectrometry. The identified peptides and analytical data are summarized in Table 2. All data for the peptide fragments had ΔC_n values greater than 0.35 and an X_{corr} values greater than 2, demonstrating good reliability. We found some peptides originating from flotillin, aquaporin1, glucose transporter 1, glycophorins, rhesus antigens, and stomatin, all of which are erythrocyte integral membrane proteins. Even peptides from low quantity membrane proteins, such as glycophorin C, were identified using this analytical method (Fig. 5 and Table 2). These findings indicate that this method is applicable to the rapid and sensitive identification of peptides from erythrocyte membrane proteins containing hydrophobic transmembrane regions.

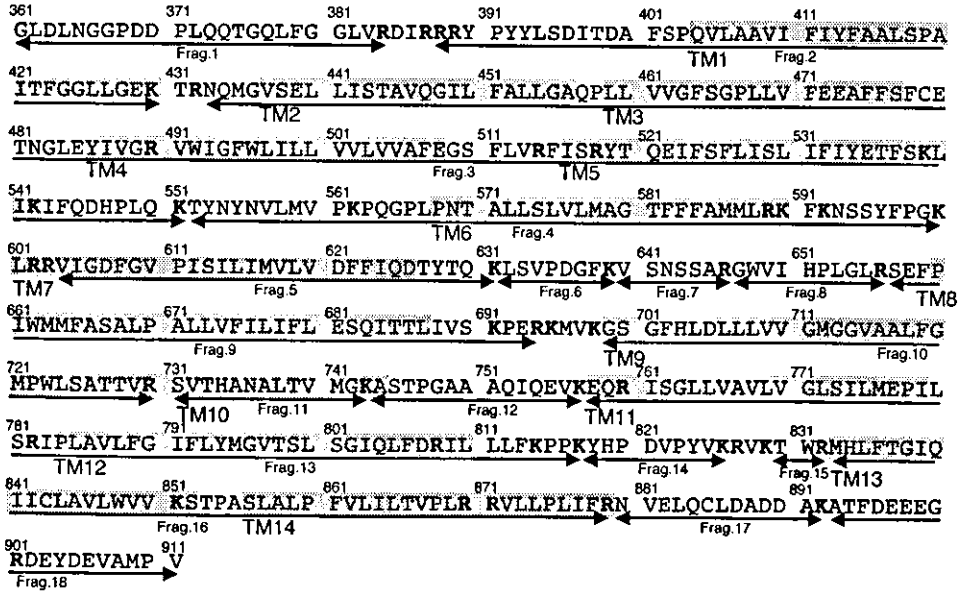

Fig. 4. **Amino acid sequence of the transmembrane domain of human band 3.** The tryptic cleavable lysines and arginines are indicated by bold type. The peptides identified by this analytical method are underlined. TM segments by hydropathic prediction (*13*) are indicated by gray boxes. The peptide fraction numbers are those in Fig. 1 and Table 1.

Table 2. **Tryptic peptide fragments of erythrocyte integral membrane proteins analyzed by LC/MS/MS systems (see text for details).**

Protein	Time (s)	*m/z*	Start	End	Sequence	ΔC_n	X_{corr}
Stomatin	9.26	1,248.40	221	232	VIAAEGEMNASR	0.502	3.268
Stomatin	24.04	1,447.65	219	232	AKVIAAEGEMNASR	0.513	3.095
Glucose transporter	31.90	1,418.60	213	223	FLLINRNEENR	0.373	3.021
Stomatin	32.48	1,931.11	126	144	VQNATLAVANITNADSATR	0.700	6.692
Glucose transporter	32.57	2,216.43	231	249	LRGTADVTHDLQEMKEESR	0.526	4.839
Glucose transporter	33.47	1,143.24	459	468	TFDEIASGFR	0.525	3.973
Glycophorin C	34.11	2,580.64	98	123	GTEFAESADAALQGDPALQDAGDSSR	0.656	5.173
Glucose transporter	34.35	1,947.08	233	249	GTADVTHDLQEMKEESR	0.497	4.287
Stomatin	35.48	1,716.99	236	251	EASMVITESPAALQLR	0.454	3.792
Glucose transporter	35.54	2,499.65	469	492	QGGASQSDKTPEELFHPLGADSQV	0.534	2.927
Aquaporin1	35.56	2,313.40	244	263	VWTSGQVEEYDLDADDINSR	0.608	4.351
Rhesus C/E antigens	36.07	1,248.38	401	409	YFDDQVFWK	0.485	2.944
Stomatin	36.11	2,029.40	233	251	ALKEASMVITESPAALQLR	0.644	5.675
Glycophorin A	36.28	3,309.56	101	131	KSPSDVKPLPSPDTDVPLSSVEIENPETSDQ	0.623	4.236
Glycophorin A	36.56	3,181.39	102	131	SPSDVKPLPSPDTDVPLSSVEIENPETSDQ	0.524	5.418
Flotillin	36.94	1,379.60	52	63	NVVLQTLEGHLR	0.480	2.722
Stomatin	37.82	1,602.87	98	111	TISFDIPPQEILTK	0.378	2.493
Glycophorin C	38.57	3,261.44	98	128	GTEFAESADAALQGDPALQDAGDSSRKEYFI	0.548	4.705
Rhesus C/E antigens	39.60	888.06	410	417	FPHLAVGF	0.564	2.014
Flotillin	40.10	1,468.84	308	321	MALVLEALPQIAAK	0.421	2.956
Stomatin	42.40	3,758.11	159	191	NLSQILSDREEIAHNMQSTLDDATDAWGIKVER	0.570	7.127
Stomatin	42.99	4,227.69	159	195	NLSQILSDREEIAHNMQSTLDDATDAWGIKVERVEIK	0.439	4.217
Glucose transporter	45.03	3,275.88	7	38	KLTGRLMLAVGGAVLGSLQFGYNTGVINAPQK[a]	0.400	3.715
Rhesus C/E antigens	45.33	2,117.41	401	417	YFDDQVFWKFPHLAVGF	0.418	3.274
Stomatin	46.89	1,756.11	78	93	GPGLFFILPCTDSFIK	0.473	2.972
Stomatin	48.45	2,128.58	264	283	NSTIVFPLPIDMLQGIIGAK	0.364	4.000
Stomatin	49.04	3,462.13	252	283	YLQTLTTIAAEKNSTIVFPLPIDMLQGIIGAK	0.403	3.849
Rhesus C/E antigens	49.37	3,098.55	235	263	KNAMFNTYYALAVSVVTAISGSSLAHPQR	0.567	3.500
Rhesus C/E antigens	51.05	2,970.37	236	263	NAMFNTYYALAVSVVTAISGSSLAHPQR	0.470	3.434
Aquaporin1	51.75	3,207.72	163	195	DLGGSAPLAIGLSVALGHLLAIDYTGCGINPAR	0.429	2.563
Rhesus antigen	54.34	2,833.28	239	264	AIVDTYFSLAACVLTAFAFSSLVEHR	0.602	2.823
Glucose transporter	54.36	3,408.93	301	333	AGVQQPVYATIGSGIVNTAFTVVSLFVVERAGR	0.489	3.376
Glucose transporter	57.76	3,124.61	301	330	AGVQQPVYATIGSGIVNTAFTVVSLFVVER	0.417	3.138
Glucose transporter	58.12	4,046.70	265	300	SPAYRQPILIAVVLQLSQQLSGINAVFYYSTSIFEK	0.525	5.275
Rhesus antigen	58.98	4,602.15	195	235	KGHENEESAYYSDLFAMIGTLFLWMFWPSFNSAIAEPGDK	0.570	4.909
Glucose transporter	59.58	2,760.45	93	127	RNSMLMMNLLAFVSAVLMGFSKLGK	0.385	3.302
Rhesus antigen	59.95	4,473.97	196	235	GHENEESAYYSDLFAMIGTLFLWMFWPSFNSAIAEPGDK	0.561	5.169
Glycophorin A	64.66	3,966.76	62	97	VQLAHHFSEPEITLIIFGVMAGVIGTILLISYGIRR	0.628	6.301
Glucose transporter	66.08	4,383.11	52	92	YGESILPTTLTTLWSLSVAIFSVGGMIGSFSVGLFVNRFGR	0.542	4.797
Glucose transporter	66.52	4,022.69	52	89	YGESILPTTLTTLWSLSVAIFSVGGMIGSFSVGLFVNR	0.393	4.265
Glycophorin A	67.65	4,449.43	62	101	VQLAHHFSEPEITLIIFGVMAGVIGTILLISYGIRRLIKK	0.509	4.102
Glycophorin A	70.73	4,321.26	62	100	VQLAHHFSEPEITLIIFGVMAGVIGTILLISYGIRRLIK	0.449	3.194
Glycophorin C	77.23	4,467.54	49	88	METSTPTIMDIVVIAGVIAAVAIVLVSLLFVMLRYMYRHK	0.584	3.066
Glycophorin B	81.86	3,996.12	55	89	FTVPAPVVIILIILCVMAGIIGTILLISYSIRRLIKA	0.441	4.149

Underlined letter indicates the transmembrane region of aquaporin 1 originating from X-ray crystallography (*3*) and other proteins predicted by the SOSUI program (*41*).

Identification of the Lysine Residues Modified by Inhibitors in Band 3—SITS and DNFB, well-known inhibitors of band 3, react covalently with lysine residues in the transmembrane region of band 3. The modified lysines have not yet been identified until now. We identified the lysines susceptible to these reagents by peptide mapping of band 3.

SITS Modified Lysine: The stilbene compounds DIDS and H_2DIDS have two isothiocyanate groups that react with amino groups in proteins. H_2DIDS reacts with Lys 539 and Lys 851 in band 3, and induces an intra-molecular cross-linkage between them (*21*). DIDS reacts with Lys 539, but no cross-link with Lys 851 is formed except under partial denaturing conditions (*24*). The other stilbene compound, SITS, has only one isothiocyanate group. Therefore, we examined which of Lys 539 or Lys 851 is more reactive toward SITS. After SITS modification and trypsin digestion, the membrane was analyzed by LC/ESI mass spectrometry. Although no molecular ions derived from fragments 1, 2, and 3 could be found, the reconstructed mass of 21,786 from the ESI mass spectrum was confirmed (Fig. 2B). To determine the SITS modified fragment, we analyzed SITS-modified membranes using the RP-HPLC system and traced the pep-

tide modified by SITS using the reference peak at a fluorescence of 430-nm (Fig. 6A). Only one peak was detected (Fig. 6A, peak a), and this peak fraction was collected and analyzed by amino acid sequencing and MALDI-TOF mass spectrometry (Table 3). The molecular mass from MALDI-TOF mass spectrometry was identical to the molecular weight identified by the LC/ESI mass. The analytical results indicate that the peptide fragment from Gly 361 to Lys 551 contains one SITS molecule, indicating that SITS modifies only Lys 539.

DNFB Modified Lysines: In the case of DNFB, two susceptible lysines are found in one band 3 molecule (*20*, *26*). Passow named these lysines Lys a and Lys c (*20*, *26*). Previous mutational analysis has suggested that Lys 539 is Lys a (*31*), however, Lys c has not yet been identified. First, to identify the 2,4-dinitrophenyl (DNP)-lysine adduct, we used LC/ESI mass spectrometry. However, the molecular ions derived from fragments 3 and 4 disappeared on the chromatogram, so that no molecular ions from peptides containing DNP-lysine adducts could be

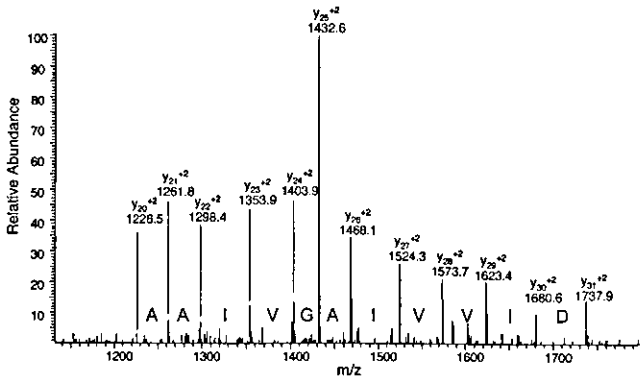

Fig. 5. **Part of the MS/MS product ion spectrum from the dissociation of the double charged molecular ion of the tryptic peptide from Met 49 to Lys 88 in glycophorin C.** The spectrum shows the sequence DIVVIAGVIAA, which corresponds to the sequence from Asp 58 to Ala 67 in glycophorin C.

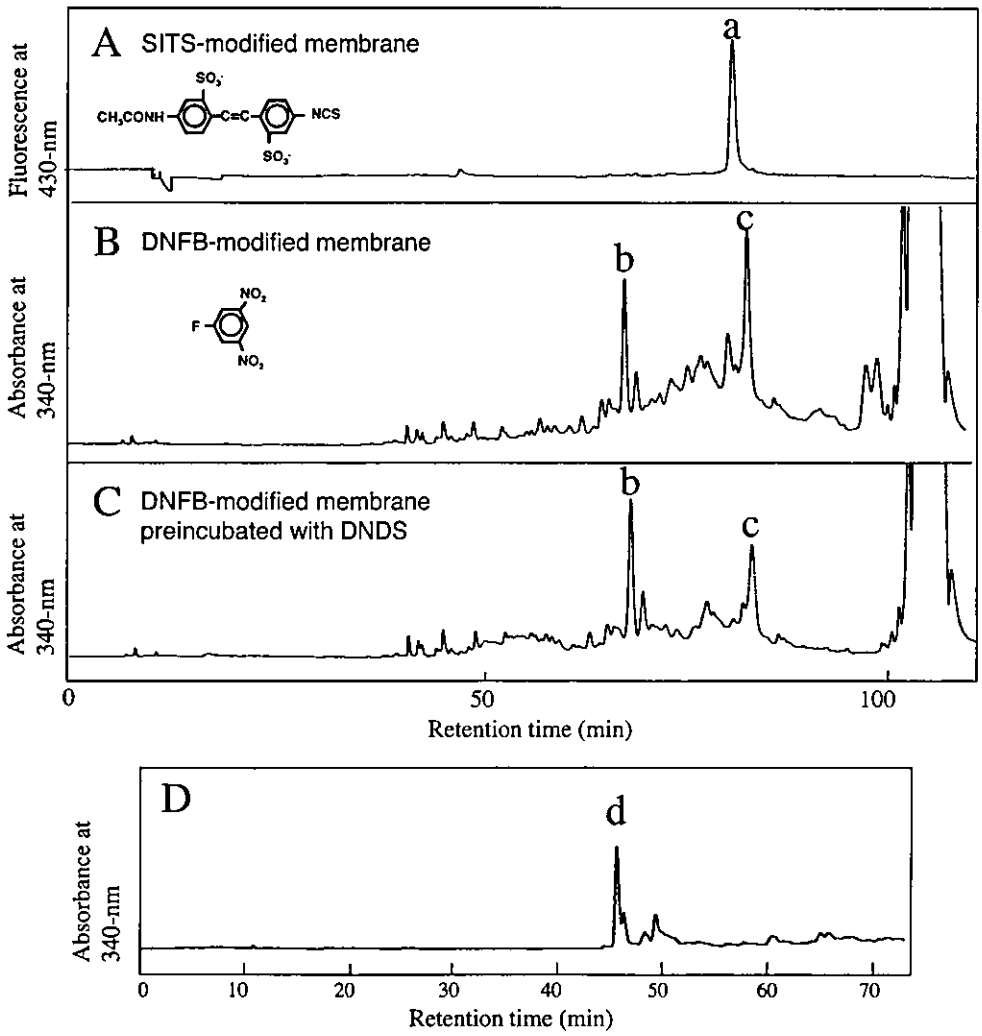

Fig. 6. **HPLC separation profiles of membranes modified by DNFB and SITS.** Membranes were modified with 0.1 mM SITS in 20 mM borate buffer, pH 9.5, at 4°C for 90 min, or with 1 mM DNFB in 20 mM Tris-HCl buffer, pH 8, at 37°C for 30 min. The modified membranes were dissolved in 0.1 M Tris-HCl (pH 8) buffer containing 0.1% $C_{12}E_8$, and digested with trypsin. The tryptic peptides in the solubilized membranes were separated by HPLC on a reverse phase column (Cosmosil 4.6 ID × 250 mm, Nakarai, Tokyo, Japan) with a water/acetonitrile/isopropanol eluent system containing 0.1% TFA as described under "MATERIALS AND METHODS." SITS-modified peptides were monitored by fluorescence at 430-nm (excitation 340-nm) and DNFB-modified peptides were monitored by absorbance at 340-nm. (A) HPLC separation profiles of tryptic peptide fragments in SITS-modified membranes. (B) HPLC separation profiles of tryptic peptide fragments in DNFB-modified membranes. (C) HPLC separation profiles of tryptic peptide fragments in DNFB-modified membrane preincubated with 100 μM DNDS for 30 min at pH 8 and 37°C. The DNFB modified peptide fraction b in (B) was collected and lyophilized. The peptide was cleaved with 10 μg CNBr in 100 μl of 50% TFA solution for 12 h at room temperature. The CNBr-treated peptides were separated by HPLC on a reverse phase column (Cosmosil 4.6 ID × 250 mm, Nakarai, Tokyo) with a water/acetonitrile/isopropanol eluent system containing 0.1% TFA as described under "MATERIALS AND METHODS." The peptides were monitored by their absorbance at 340 nm. The HPLC separation profile of the CNBr cleavage fragments is shown in D). The peak fractions a, b, c, and d were analyzed by MALDI-TOF mass spectrometry and amino acid sequencing, and the results are summarized in Table 3.

Table 3. **Peptide analyses of peptides from SITS- and DNFB-modified membranes.**

Peak	The observed mass[a]	Amino acid sequencing	The identified peptide fragment
Fig. 6a	21,787.0	GLDLNG	Gly 361 to Lys 551 (predicted mass, 21,334) containing one SITS (molecular weight 452) molecule
Fig. 6b	5,712.54	TYNYNV	Thr 552 to Lys 600 (predicted mass, 5,546.7) containing one DNP (molecular weight 167) molecule
Fig. 6c	13,669.9	NQMGVS	Asn 433 to Lys 551 (predicted mass, 13,504) containing one DNP molecule
Fig. 6d	1,739.24	LRXFKN[b]	Leu 588 to Lys 600 (predicted mass, 1,571.87) containing one DNP molecule and Lys 590 modified with DNFB

[a]Mass of a single charged ion by MALDI-TOF mass spectrometry. [b]The third PTH-amino acid was not detectable.

found. Therefore, we analyzed DNFB-modified membranes using the RP-HPLC system and traced the peptide modified by DNFB using the reference peak at 340-nm absorbance (Fig. 6B). We observed two main peaks at 63 min (Fig. 6B, peak b) and 80 min (Fig. 6B, peak c), and these peak fractions were collected and analyzed (Table 3). Analysis of peak b suggested that a fragment from Thr 552 to Lys 600 contains one DNP molecule. This peptide fragment contains three possible lysines, at positions 562, 590, and 592, that are susceptible to DNFB. To identify the DNFB-susceptible lysine, we carried out CNBr treatment of this fragment. Figure 6D shows the HPLC profile of the CNBr treated fragments. The peak d fraction was collected and analyzed. The peptide molecular weight of was 1739.24 and was estimated to comprise the region from Leu 588 to Lys 600, containing one DNP molecule (Table 3). The N-terminal sequence was LRXFKN and level of the 3rd PTH-lysine was diminished. These results indicate that Lys 590 is modified by DNFB. Peak c comprised the region from Asn 433 to Lys 551 and contained one DNP molecule (Table 3). Preincubation with 100 μM of the non-covalent binding stilbene compound DNDS resulted in a decrease in the intensity of peak c (Fig. 6D). This is consistent with previous findings of competition between DNFB and H_2DIDS for reaction with Lys 539 (*26*). Therefore, we determined that Lys c is Lys 590, further supporting the identity of Lys a as Lys 539.

DISCUSSION

In the present study, we applied a peptide analytical method to tryptic fragments of erythrocyte membrane proteins. Using this method, we could analyze peptides originating from the 55-kDa band 3 transmembrane domain (Gly 361–Val 911) and other erythrocyte integral membrane proteins (see Figs. 1–5, Tables 1 and 2). This method has many advantages for the study of erythrocyte membrane proteins. First, the membrane proteins can be solubilized in mild detergent and digested with protease under mild conditions. Second, peptides can be analyzed rapidly using LC/ESI mass spectrometry. These factors are useful for the determination of the residues modified by unstable chemical reagents. In our recent study, we determined the DEPC-modified histidine that is important for the anion transport mechanism of band 3 (*23*). DEPC histidine adducts are easily hydrolyzed (*32*); however, we could overcome this obstacle by using mild conditions and rapid analysis.

The greatest advantage of this method is its ability to analyze directly peptides and proteins originating from intact erythrocyte membranes. Furthermore, we identified most peptides in the band 3 transmembrane domain (97% of sequence). Therefore, the method allowed us to determine band 3 residues susceptible to certain chemical modifications directly. In previous chemical modification studies, lysine, arginine, glutamic acid and histidine residues have been shown to be essential for transport activity (*16–23*).

SITS and DNFB are lysine specific reaction reagents and anion transport inhibitors. In this study, we determined that lysine 539 is susceptible to SITS and lysines 539 and 590 are susceptible to DNFB using peptide mapping of band 3. SITS is a well-known and well-studied inhibitor of band 3 anion transport, and the predominant modified lysine has been assumed to be Lys 539 base on studies of other stilbene compounds bound to band 3 (*21*, *24*). In the case of DNFB, Lys 539 had been identified as one modification site (*31*); however, here we provide the first evidence that Lys 590 is another DNFB modification site. The inhibition of anion transport depends on SITS and DNFB modification of Lys 539, which is the main reaction site of other lysine-reactive inhibitors, for example, stilbene compounds including DIDS and H2DIDS (*21*, *24*). The sites must not be anion binding sites within the anion exchange center, because the mouse band 3 mutant K558N, which corresponds to K539N of human band 3, has the same specific activity as wild-type band 3 in *Xenopus oocytes* (*18*). Thus, we conclude that Lys 539 is part of the extracellular rim of the anion transport channel (*20*). While the transport activity of band 3 is slightly increased by the DNFB modification of Lys 590 (*26*), Lys 590 is also the site modified by phenylisothiocyanate, which modifies three lysines in the band 3 molecule (*33*). Interestingly, modification by phenylisothiocyanate leads to an inhibition of the anion transport activity of band 3 (*33*). Therefore, Lys 590 plays a role in regulating the transport activity of band 3. Passow *et al.* examined the anion effect of DNFB modification of two lysines (*20*). They found that when Lys 590 is modified by DNFB, the rate of DNFB modification at Lys 539 is reduced in chloride medium but not in sulfate medium. When Lys 590 is modified by DNFB, the rate of DNFB modification at Lys 539 is slightly faster in sulfate medium than in chloride medium. On the other hand, when Lys 590 is free, the rate of DNFB modification at Lys 539 is about 10 fold faster in chloride medium than in sulfate medium. These complex results in different anions media indicate that two lysines undergo allosteric interactions with the anion binding site (*20*). The regulation of anion transport activity and the allosteric interactions with the anion binding site indicate that Lys 590 is located on the same part of the anion transport channel as Lys 539.

Transmembrane segment containing Lys 590 (TM 6) are resistant to proteases in the native conformation;